

Online Multivariate Change-point Detection: Leveraging Links With Computational Geometry

Liudmila Pishchagina¹, Gaetano Romano², Paul Fearnhead², Vincent Runge¹,
and Guillem Rigail^{*1,3,4}

¹Université Paris-Saclay, CNRS, Univ Evry, Laboratoire de Mathématiques et Modélisation d'Evry, 91037, Evry-Courcouronnes, France.

²School of Mathematical Sciences, Lancaster University, Lancaster LA1 4YF, UK

³Université Paris-Saclay, CNRS, INRAE, Univ Evry, Institute of Plant Sciences Paris-Saclay (IPS2), 91405, Orsay, France.

⁴Université Paris-Saclay, AgroParisTech, INRAE, UMR MIA Paris-Saclay, 91120, Palaiseau, France.

Abstract

The increasing volume of data streams poses significant computational challenges for detecting change-points online. Likelihood-based methods are effective, but a naive sequential implementation becomes impractical online due to high computational costs. We develop an online algorithm that exactly calculates the likelihood ratio test for a single change-point in p -dimensional data streams by leveraging a fascinating connection with computational geometry. This connection straightforwardly allows us to exactly recover sparse likelihood ratio statistics: that is assuming only a subset of the dimensions are changing. Our algorithm is straightforward, fast, and apparently quasi-linear. A dyadic variant of our algorithm is provably quasi-linear, being $\mathcal{O}(n \log(n)^{p+1})$ for n data points and p less than 3, but slower in practice. These algorithms are computationally impractical when p is larger than 5, and we provide an approximate algorithm suitable for such p which is $\mathcal{O}(np \log(n)^{\tilde{p}+1})$, for some user-specified $\tilde{p} \leq 5$. We derive statistical guarantees for the proposed procedures in the Gaussian case, and confirm the good computational and statistical performance, and usefulness, of the algorithms on both empirical data and NBA data.

Keywords: computational geometry, convex hull, dynamic programming, online change-point detection

*Corresponding author: guillem.rigail@inrae.fr

1 Introduction

In recent years, many methods have been proposed for detecting one or multiple changepoints offline or online in data streams. The reason for such a keen interest in changepoint detection methods lies in its importance for various real-world applications, including bioinformatics [Olshen et al., 2004, Picard et al., 2005], econometrics [Bai and Perron, 2003, Aue et al., 2006], medicine [Bosc et al., 2003, Staudacher et al., 2005], climate and oceanography [Ducre-Robitaille et al., 2003, Reeves et al., 2007], finance [Andreou and Ghysels, 2002, Fryzlewicz, 2014], autonomous driving [Galceran et al., 2017], entertainment [Rybach et al., 2009, Radke et al., 2005], computer vision [Ranganathan, 2012] or neuroscience [Jewell et al., 2022]. Whether this is online (i.e. observations are processed as they become available) or offline (i.e. observations are processed only once the whole data is available) the ever-increasing size of the data stream raises computational challenges. Ideally, a changepoint procedure should be linear or quasi-linear in the size of the data and, for online applications, should also be able to process new observations sequentially, and as quickly as they arrive. A common idea for both offline and online parametric (multiple) changepoint model estimation, is to optimise a likelihood function or calculate likelihood ratio statistics [Siegmund and Venkatraman, 1995, Auger and Lawrence, 1989]. From a computational perspective this optimisation can either be done (1) heuristically using, for example, the Page-CUSUM statistic [Page, 1954] in an online context or Binary Segmentation and its variants [Scott and Knott, 1974, Fryzlewicz, 2014] in an offline context, or (2) exactly using dynamic programming techniques as in the Segment Neighbourhood, or Optimal Partitioning algorithms [Auger and Lawrence, 1989, Jackson et al., 2005]. Importantly, these later algorithms used with an appropriate penalty enjoy good statistical properties [Yao, 1984, Lavielle and Moulines, 2000, Lebarbier, 2005, Garreau and Arlot, 2017] and have shown good properties in numerous applications [Lai et al., 2005, Liehrmann et al., 2021].

Significant speed-ups are possible by reducing the set of changepoint locations that need to be checked at each iteration of the dynamic programming recursion, a technique commonly known as pruning [Killick et al., 2012, Rigaiil, 2015, Maidstone et al., 2017, Romano et al., 2023]. Two types of rules have been proposed that prune changepoint locations that will never contribute to the full optimisation cost, achieving significant speed-ups without sacrificing optimality. Inequality pruning rules, as in the PELT algorithm [Killick et al., 2012], apply to a wide range of changepoint models but are efficient only if the number of true changepoints increases quickly with the size of the data. Functional pruning, as in the pDPA, FPOP, or FOCuS algorithms [Rigaiil, 2015, Maidstone et al., 2017, Romano et al., 2023], applies mostly to univariate models, but is efficient even when the number of true changepoints is small compared to the size of the data. Interestingly, these algorithms are sequential in nature and empirically quasi-linear. This quasi-linearity was recently proven for the online detection of a single changepoint [Romano et al., 2023]. The pDPA, FPOP, and FOCuS algorithms rely on a functionalisation of the problem, that is they consider the likelihood as a function of the last segment parameter. A direct extension of these ideas to a higher dimension ($p > 1$) has proven difficult because it involves computing the intersection and subtraction of many convex sets in \mathbb{R}^p [Runge, 2020, Pishchagina et al., 2023].

In this paper, we study online models with one changepoint, where the likelihood can be algebraically written as a log-likelihood from the p -variate natural exponential family.

This includes, for example, the Gaussian, Poisson, categorical, and Pareto type-I distribution (assuming the minimum value is known) and also the non-parametric e-detectors of Shin et al. [2022] (see Section 5). We extend the functional pruning approach to such p -variate models using a linearisation argument embedding all likelihoods into a bigger space of dimension $p+2$. This idea allows us to demonstrate a link between the functional problem and problems studied in computational geometry.

In particular, we show that the solutions of this extension correspond to identifying the supporting hyperplanes of a particular half-space intersection problem. For models with one changepoint, we demonstrate that this problem further simplifies and is dual to a lower dimensional convex hull problem of dimension $p + 1$. In this latter case, we further prove, assuming independent and identically distributed (i.i.d.) data, that the number of points on this hull at time n is asymptotically $\mathcal{O}(\log^p(n))$. Leveraging this leads to an empirically log-linear per iteration algorithm for calculating the likelihood ratio test statistics for a change at t .

At any time-step of this algorithm, we can exactly compute the maximum likelihood ratio-statistics and maximum sparse likelihood ratio-statistics allowing only s coordinates to change with $s \leq p$. In Supplementary Material I, we derive non-asymptotic bounds of these statistics to control the false alarm rate and derive a bound on the expected detection delay. While the computational cost is quasi-linear, our exact algorithms become impractical for large p , due to the $\log^p(n)$ scaling. For such cases we

provide an approximation storing only an order of $\mathcal{O}(p \log^{\tilde{p}}(n))$ candidates on the hull, where $\tilde{p} \leq p$, chosen by the user, represents the dimension of a projective linear space.

The paper has the following structure. Section 2 describes our maximum likelihood framework. Section 3 presents the mathematical formulation of the functional pruning problem and how it is related to a half-space intersection problem and a convex hull problem. In Section 4 we develop and introduce our proposed method, called MdFOCuS, together with an approximation that scales to larger values of p . An important feature of both algorithms is that they calculate sets of putative changepoint locations. Given such a set it is straightforward to maximise the test statistic of interest, including under constraints on the number of components that change, or allowing different models for different components. We provide statistical guarantees of the resulting test in the Gaussian setting and compare MdFOCuS with competitor algorithms in terms of statistical and computational efficiency – showing its increased accuracy when the pre-change parameters are unknown. In Section 5 we apply our methodology to track the performances of an NBA team and discuss how our theory could accelerate the recently proposed non-parametric e-detectors [Shin et al., 2022]. All proofs, and links to code for this paper, are given in the Supplementary Material.

2 Maximum Likelihood Methods for Online Single Changepoint Detection

2.1 Problem set-up

We consider observations $\{y_t\}_{t=1,2,\dots}$ in \mathbb{R}^p and wish to detect the possible presence of a changepoint and estimate its location. If there is a change, we denote the time of the change

as τ . We will consider likelihood-based approach that postulates a model for the data in the segments before and after the changepoint. Our model will be that the data point y_t is i.i.d. from a distribution with density $f_Y(y_t|\theta_1)$ before the change and $f_Y(y_t|\theta_2)$ after the change.

At time n , twice the log-likelihood for the time series $\{y_t\}_{t=1,\dots,n}$, in terms of the pre-changepoint parameter, θ_1 in $\mathbb{R}^{p''}$, the post-changepoint parameter, θ_2 in $\mathbb{R}^{p''}$, and the location of a change, τ , is

$$\ell_{\tau,n}(\theta_1, \theta_2) = 2 \left(\sum_{t=1}^{\tau} \log f_Y(y_t|\theta_1) + \sum_{t=\tau+1}^n \log f_Y(y_t|\theta_2) \right). \quad (1)$$

Depending on the application one may assume that the pre-changepoint parameter θ_1 is either known or unknown. In either case, we can get the log-likelihood for a changepoint at τ by maximising this equation over either the unknown parameter, θ_2 , or parameters, θ_1 and θ_2 . In practice, we do not know the changepoint location, so we maximise this log-likelihood over τ . We can define the maximum likelihood estimator for τ , for the pre-changepoint parameter being either known or unknown respectively, as

$$\begin{aligned} \hat{\tau}(\theta_1) &= \arg \max_{\tau} (\max_{\theta_2} \ell_{\tau,n}(\theta_1, \theta_2)), \\ \hat{\tau}(\cdot) &= \arg \max_{\tau} (\max_{\theta_1, \theta_2} \ell_{\tau,n}(\theta_1, \theta_2)). \end{aligned}$$

We then obtain a Generalized Likelihood Ratio (GLR) statistic [Siegmund and Venkatraman, 1995] for a change τ by comparing it with twice the log-likelihood for a model with no change. That is $2 \sum_{t=1}^n \log f_Y(y_t|\theta_1)$ if θ_1 is known and $\max_{\theta_1} 2 \sum_{t=1}^n \log f_Y(y_t|\theta_1)$ if it is not. Often it is appropriate [see, for example, Chen et al., 2022] to consider a sparse version of the likelihood that allows only s coordinates to jump, that is adding the constraint $s = \|\theta_1 - \theta_2\|_0$, where $\|\mathbf{v}\|_0$ is equal to the number of non-zero entries of \mathbf{v} . The estimator of τ in this case, assuming the pre-change mean is known, is

$$\hat{\tau}^s(\theta_1) = \arg \max_{\tau} \left(\max_{\substack{\theta_2 \\ \|\theta_1 - \theta_2\|_0 = s}} \ell_{\tau,n}(\theta_1, \theta_2) \right), \quad (2)$$

with $\hat{\tau}^s(\cdot)$ defined analogously for the case where the pre-change mean is unknown. Clearly, $\hat{\tau}^p(\theta_1) = \hat{\tau}(\theta_1)$ and $\hat{\tau}^p(\cdot) = \hat{\tau}(\cdot)$.

Offline, optimising Equation (1) is simple. Indeed, assuming we have access to all the data, it suffices to compute, for every possible changepoint location from 1 to $n - 1$, the likelihood (which can be done efficiently using summary statistics) and then pick the best value. Online, the problem is substantially more difficult as one needs to recompute the maximum for every new observation. Applying the previous offline strategy for every new observation is inefficient as it takes a computational cost of order n to process the n th observation. It is infeasible for an online application, where n grows unbounded, and for this reason, various heuristic strategies have been proposed [see Wang and Xie, 2022, for a recent review]. From a computational perspective, we roughly identify two main types of heuristics. The first idea is to restrict the set of possible (θ_1, θ_2) pairs to be discrete. The simplest case is to consider just one pair of (θ_1, θ_2) as in the Page CUSUM strategy [Page,

1954], but one typically considers a grid of values [Chen et al., 2022]. The second idea is to restrict the set of changepoint locations one considers. For example, to consider a grid of window lengths w_1, \dots, w_M and at time n compute the GLR statistic only for changes at $\tau = n - w_1, \dots, n - w_M$ [Eiauer and Hackl, 1978, Meier et al., 2021]. But this naturally introduces a trade-off between computational efficiency and statistical power: the larger the grid of windows, the larger the computational overhead [Wang and Xie, 2022].

Recently, the FOCuS algorithm has been introduced that calculates the GLR test exactly but with a per-iteration cost that increases only logarithmically with the amount of data [Romano et al., 2023, Ward et al., 2023] - however, this algorithm is only applicable for detecting changes in a univariate feature of a data stream. A key insight from the FOCuS algorithm is that to maximise the likelihood, one only needs to consider changes that correspond to points on a particular convex hull in the plane. This link to geometrical features of the data is one that we leverage to develop algorithms for detecting changes in multivariate features.

2.2 Detection of a single change in the parameter of a distribution in the exponential family

We briefly introduce some notation. We use $\mathbf{1}_p$ to denote a vector of length p in which all elements are set to one. For any vector $\mu = (\mu^1, \dots, \mu^p)$ in \mathbb{R}^p , we define its q -norm as $\|\mu\|_q := (\sum_{k=1}^p |\mu^k|^q)^{1/q}$, where $q \geq 1$ in \mathbb{R} . For two vectors, $\mu_1 = (\mu_1^1, \dots, \mu_1^p)$ and $\mu_2 = (\mu_2^1, \dots, \mu_2^p)$ in \mathbb{R}^p , we define their scalar product as $\langle \mu_1, \mu_2 \rangle = \sum_{k=1}^p \mu_1^k \mu_2^k$. The symbol $|\cdot|$ signifies the cardinality of \cdot .

We are now ready to describe our model. We assume that the density $f_Y(y_t|\theta_k)$, for observation y_t in segment $k \in \{1, 2\}$ which has segment-specific parameter θ_k , can be written in the form

$$f_Y(y_t|\theta_k) = \exp \left\{ -\frac{1}{2} (A'(r(\theta_k)) - 2\langle s(y_t), r(\theta_k) \rangle + B'(s(y_t))) \right\}, \quad (3)$$

where s and r are functions mapping respectively the observations, y_t , and the parameters, θ_k , to \mathbb{R}^p , A' is some convex function from \mathbb{R}^p to \mathbb{R} , and B' from \mathbb{R}^p to \mathbb{R} . Defining the natural parameter η_k as $\eta_k = r(\theta_k)$, and x_t as $x_t = s(y_t)$ we rewrite this density as a function of η_k and x_t :

$$f_X(x_t|\eta_k) = \exp \left\{ -\frac{1}{2} (A'(\eta_k) - 2\langle x_t, \eta_k \rangle + B'(x_t)) \right\}. \quad (4)$$

This class encompasses many common exponential family models, see Table 4 in the Supplementary Material. There, we also show how a change in mean and variance of a Gaussian signal in \mathbb{R} can be expressed in this form.

We can then define the log-likelihood of our (transformed) data x_1, \dots, x_t , under a model with a change at τ in terms of η_1 and η_2 as

$$\ell_{\tau,n}(\eta_1, \eta_2) = - \sum_{t=1}^{\tau} [A'(\eta_1) - 2\langle x_t, \eta_1 \rangle + B'(x_t)] - \sum_{t=\tau+1}^n [A'(\eta_2) - 2\langle x_t, \eta_2 \rangle + B'(x_t)]. \quad (5)$$

The log-likelihood estimator for τ , for the pre-change parameter being either known or unknown respectively, is

$$\hat{\tau}(\eta_1) = \arg \max_{\tau} (\max_{\eta_2} \ell_{\tau,n}(\eta_1, \eta_2)), \text{ or } \hat{\tau}(\cdot) = \arg \max_{\tau} (\max_{\eta_1, \eta_2} \ell_{\tau,n}(\eta_1, \eta_2)).$$

The GLR statistic for a change τ is obtained by comparing with $\sum_{t=1}^n [A'(\eta_1) - 2\langle x_t, \eta_1 \rangle + B'(x_t)]$ if η_1 is known and with $\max_{\eta_1} \sum_{t=1}^n [A'(\eta_1) - 2\langle x_t, \eta_1 \rangle + B'(x_t)]$ if it is not.

For any fixed η_1 and any η_2 the addition of $\sum_{t=1}^n [A'(\eta_2) - 2\langle x_t, \eta_2 \rangle + B'(x_t)]$ to (5) does not change $\arg \max_{\tau} \ell_{\tau,n}(\eta_1, \eta_2)$. Moreover, this addition eliminates the dependence on n . Hence, when searching for the maximum likelihood change, we can redefine $\ell_{\tau,n}(\eta_1, \eta_2)$ as follows:

$$\ell_{\tau}(\eta_1, \eta_2) = \tau [A'(\eta_2) - A'(\eta_1)] - 2 \left\langle \sum_{t=1}^{\tau} x_t, \eta_2 - \eta_1 \right\rangle, \quad (6)$$

and be sure that the optimal change optimises $\ell_{\tau}(\eta_1, \eta_2)$ at least for a pair (η_1, η_2) . Sometimes it might make sense to regularise the parameters. This can be done by adding a function of the parameter $\Omega(\eta_1, \eta_2)$, such as $\Omega(\eta_1, \eta_2) = \lambda(\|\eta_1\|_1 + \|\eta_2\|_1)$ for some $\lambda > 0$, to (5). We will not study this further, but by the previous addition trick, any such regularisation term could be subtracted, and the rest of our argument would hold.

Throughout, we will primarily focus on the case where η_1 is known. Our results for the case where it is unknown are derived as a by-product: considering all possible η_1 simultaneously and realising they all lead to the same geometrical problem. Considering η_1 to be fixed we thus introduce the following definitions: $\mu = \eta_2 - \eta_1$, $A(\mu) = A'(\mu + \eta_1) - A'(\eta_1)$, and rewrite the function $\ell_{\tau}(\eta_1, \eta_2)$ as a function of μ :

$$\ell_{\tau}(\mu) = \tau A(\mu) - 2 \left\langle \sum_{t=1}^{\tau} x_t, \mu \right\rangle. \quad (7)$$

3 Linear Relaxation of the Functional Pruning Problem

3.1 Mathematical Formulation

Functional pruning ideas give the potential of an efficient approach to recursively calculate the GLR statistic for a change at time $n + 1$ given calculations at time n [Romano et al., 2023]. The idea is to restrict the set of possible changepoints prior to $n + 1$ that we need to consider. Working out which changepoint locations we need to consider is obtained by viewing the GLR statistic as a function of the change parameter $\mu = \eta_2 - \eta_1$, and finding the set of changepoint locations which contribute to this, i.e. for which the GLR statistic is maximum for some value of μ .

In more detail, at step n of a functional pruning algorithm, we consider a list of possible changepoints τ of the data from $x_1, x_2 \dots$ to x_n . Each changepoint is represented by a function f_{τ} of the last segment parameter μ and a set of μ values for which it is maximising the likelihood: $Set_{\tau} = \{\mu \mid \forall \tau' \neq \tau, f_{\tau}(\mu) > f_{\tau'}(\mu)\}$. To proceed to the next data point $n + 1$ the update is informally done as follows.

1. We add n to the list of changepoints, with this represented by a function f_n .

2. We compare all other functions to this new function and accordingly restrict the set of μ for which they are optimal.
3. We discard all changepoints whose set Set_τ is empty.

The left column of Figure 1 provides a graphical representation of these steps. The pruning of the third step is valid because, whatever the data points after $n + 1$ might be, these functions (or equivalently changepoints) can never maximise the log-likelihood. Formally, define functions f_τ , for τ in some set \mathcal{T} , such that

$$f_\tau(\mu) = a_\tau A(\mu) - 2\langle b_\tau, \mu \rangle, \quad (8)$$

where a_τ is in \mathbb{R} , and b_τ is in \mathbb{R}^p and A is a convex function from \mathcal{D}_A , a subset of \mathbb{R}^p . We define $Im(A)$ as the image of the function A . Function f_τ corresponds to the log-likelihood for a segmentation with a change at τ and with parameter μ . This function will depend on μ through the log-likelihood contribution of the data in the segment after τ , with this data defining the co-efficients a_τ and b_τ . We then define

$$F_{\mathcal{T}}(\mu) = \max_{\tau \in \mathcal{T}} \{f_\tau(\mu)\},$$

and our goal is to recover all the indices τ maximising $F_{\mathcal{T}}$ for at least one value of μ . Define:

$$\mathcal{F}_{\mathcal{T}} = \{\tau \mid \exists \mu \in \mathcal{D}_A \subset \mathbb{R}^p, \forall \tau' \in \mathcal{T} \text{ with } \tau' \neq \tau : f_\tau(\mu) > f_{\tau'}(\mu)\}. \quad (9)$$

This is defined using a strict inequality. As function A is strictly convex, (and assuming that for all $\tau \neq \tau'$ we cannot have simultaneously $a_\tau = a_{\tau'}$ and $b_\tau = b_{\tau'}$) equality can be obtained only over a set of zero measure, and can be ignored.

3.2 Linearisation of the Functional Pruning Problem

The size of the set $\mathcal{F}_{\mathcal{T}}$ depends on the nature of the function A . In essence, to consider any possible function A , we introduce a new parameter λ to replace $A(\mu)$. This way we get a problem that does not depend on the form of A and, as we will see, is easier to solve, albeit at the cost of an additional dimension. To be specific, for any function $\mu \mapsto f_\tau(\mu)$ we associate an (augmented) function $(\lambda, \mu) \mapsto g_\tau(\lambda, \mu)$ defined as:

$$g_\tau(\lambda, \mu) = a_\tau \lambda - 2\langle b_\tau, \mu \rangle.$$

As for the f_τ , we define the maximum $G_{\mathcal{T}}(\lambda, \mu)$ as

$$G_{\mathcal{T}}(\lambda, \mu) = \max_{\tau \in \mathcal{T}} \{g_\tau(\lambda, \mu)\}.$$

Again our goal will be to recover the index τ strictly maximising $G_{\mathcal{T}}$:

$$\mathcal{G}_{\mathcal{T}} = \{\tau \mid \exists (\lambda, \mu) \in Im(A) \times \mathcal{D}_A, \forall \tau' \in \mathcal{T} \text{ with } \tau' \neq \tau : g_\tau(\lambda, \mu) > g_{\tau'}(\lambda, \mu)\}.$$

In the previous definition, the parameter λ is constrained to be in the image of the function A . The values attained by f_τ are also attained by g_τ on a parametric curve of the (λ, μ) space given by equation $\lambda = A(\mu)$, so that $f_\tau(\mu) = g_\tau(A(\mu), \mu)$. This trivially leads to the following result that the set of τ strictly maximising $\mathcal{G}_{\mathcal{T}}$ must contain the set strictly maximising $\mathcal{F}_{\mathcal{T}}$.

Theorem 1. $\mathcal{F}_{\mathcal{T}} \subseteq \mathcal{G}_{\mathcal{T}}$.

Without any further assumptions on the function A , the set $\mathcal{G}_{\mathcal{T}}$ could be much larger than $\mathcal{F}_{\mathcal{T}}$. The following theorem demonstrates that equality holds for an important class of functions $A(\mu)$.

Theorem 2. *If $A(\mu) = \|\mu\|^q$ with $q > 1$, then $\mathcal{F}_{\mathcal{T}} = \mathcal{G}_{\mathcal{T}}$.*

In particular, with $q = 2$ we get the Gaussian loss function with $\eta_1 = 0$. Assuming $\eta_1 = 0$ is not restrictive because if η_1 is not 0 we can consider the translated data $(x_t - \eta_1)$. A more general result, with milder conditions for function A , is proposed in Supplementary Material D. One sufficient condition consists of the strong convexity of the function A with $A(0) = 0$.

3.3 Half-space intersections and functional pruning

All g_{τ} functions are linear in (λ, μ) . Considering yet another variable κ we can associate to every g_{τ} a function h_{τ} and a half-space H_{τ} of \mathbb{R}^{p+2} :

$$H_{\tau} = \{\kappa, \lambda, \mu \mid h_{\tau}(\kappa, \lambda, \mu) = a_{\tau}\lambda - 2\langle b_{\tau}, \mu \rangle - \kappa \leq 0\}.$$

From here we straightforwardly get that our linearised functional problem is included in a half-space intersection problem. This result is formalised in the following theorem.

Theorem 3. *If τ is in $\mathcal{G}_{\mathcal{T}}$ then*

1. *there exists (κ, λ, μ) such that $h_{\tau}(\kappa, \lambda, \mu) = 0$ and for all $\tau' \neq \tau$, $h_{\tau'}(\kappa, \lambda, \mu) < 0$;*
2. *$h_{\tau}(\kappa, \lambda, \mu) = 0$ defines a supporting hyperplane of the set $\cap_{\tau} H_{\tau}$.*

The set $\cap_{\tau} H_{\tau}$ defines an unbounded polyhedron as taking any $\kappa \geq \max_{\tau} \{c_{\tau}\}$, $\lambda = 0$, and $\mu = 0$ we solve all inequalities. In Figure 1 we illustrate our linearised functional problem.

Computing the intersection of $|\mathcal{T}|$ half-spaces is a well-studied problem in computational geometry. It is closely related to the convex hull problem by projective duality [Avis and Bremner, 1995], and several algorithms have been proposed [see for example Preparata and Muller, 1979, Brondsted, 1983, Barber et al., 1996, O'Rourke, 1998]. See Seidel [2017] for a recent short introduction to this topic.

3.4 Projective-duality

The following theorem states that in our case the half-space intersection problem in dimension $p + 2$ is dual to a convex hull problem in dimension $p + 1$.

Theorem 4. *An index τ being in $\mathcal{G}_{\mathcal{T}}$ is equivalent to the point (a_{τ}, b_{τ}) in \mathbb{R}^{p+1} being a vertex of the convex hull of $\{(a_{\tau}, b_{\tau})\}_{\tau \in \mathcal{T}}$.*

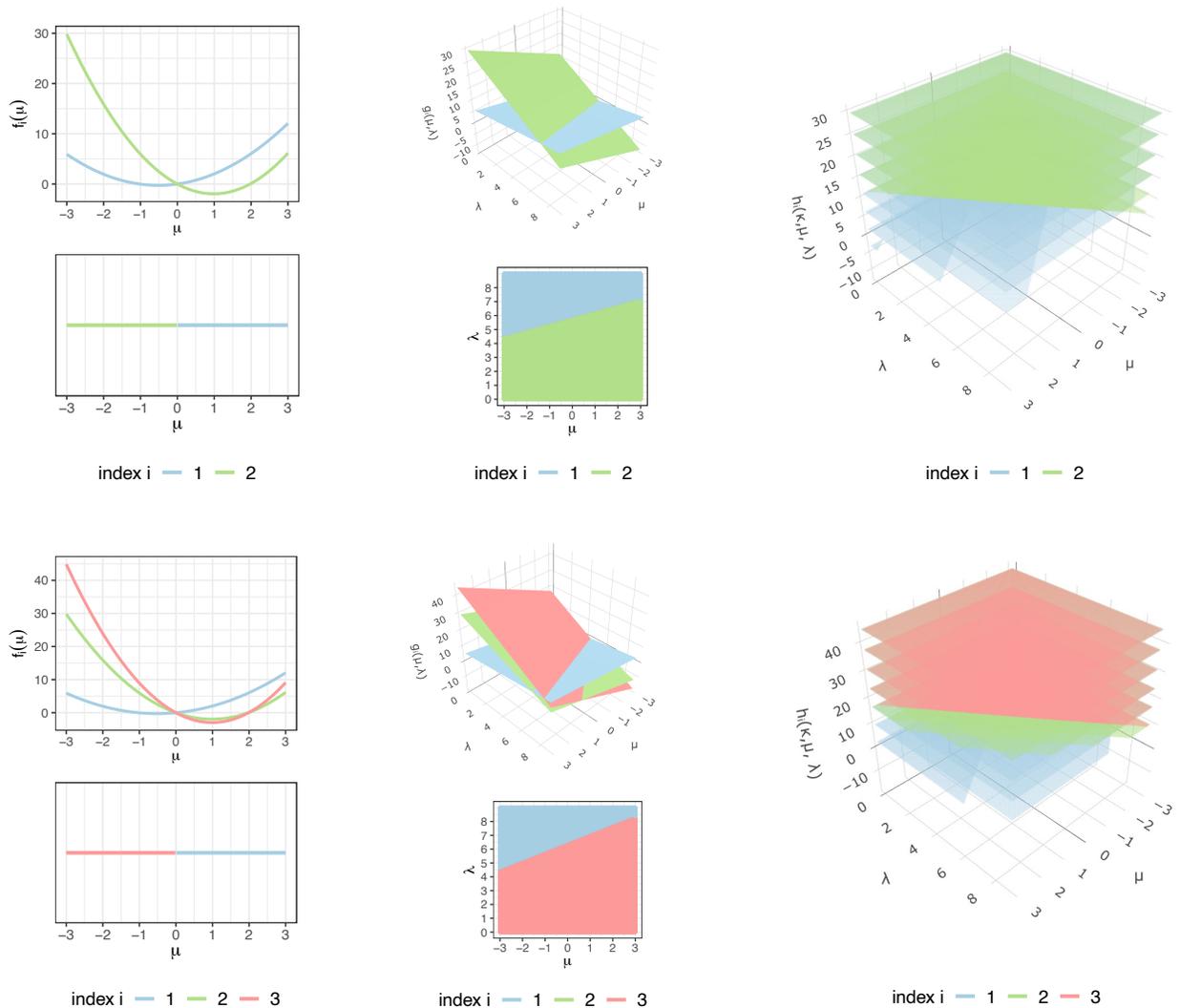


Figure 1: Example of the functional pruning problem and linearised functional problem over times: f_i and $\text{proj}\{\max_i\{f_i(\mu)\}\}$ functions (left); g_i and $\text{proj}\{\max_i\{g_i(\mu, \lambda)\}\}$ functions (middle); the level surfaces of h_i functions, where each surface is for a fixed κ value (right) for changepoint candidates $i \in \mathcal{T}$. We simulate time series $\{x_t\}_{t=1,2,\dots} \sim \mathcal{N}(0, 1)$ and consider two time-steps, $n = 3$ (top two rows) and $n = 4$ (bottom two rows). We define the coefficients a_i as i , b_i as $\sum_{t=1}^i x_t$. The change $i = 2$ associated with quadratics f_2 and surface g_2 is pruned at $n = 4$.

We illustrate the points on the convex hull of Theorem 4 for $p = 1$ and $p = 2$ in Figure 2. As will be seen in Section 4, this is relevant for the online detection of a single changepoint, see (7). Importantly, computing the convex hull of $|\mathcal{T}|$ points is a well-studied problem in computational geometry. Over the years many algorithms have been developed [Chand and Kapur, 1970, Preparata and Hong, 1977, Miller and Stout, 1988, Barber et al., 1996, Kenwright, 2023]. In the rest of this paper, we will use the `QuickHull` algorithm of Barber

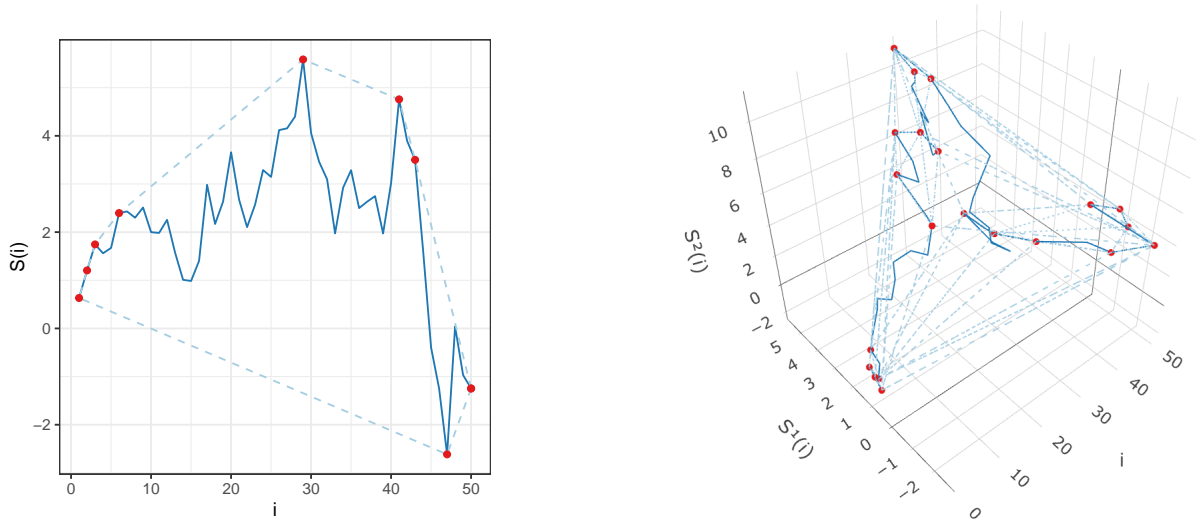


Figure 2: Plot of $S(i) = \sum_{t=1}^i x_t$ as a function of i (dark blue) and the convex hull of $\{(a_i = i, b_i = S(i))\}_{i \in \{1, \dots, n-1\}}$ (dashed blue line) for dimensions $p = 1$ (left) and 2 (right). The vertices of the convex hull $\tau \in \mathcal{T}$ are marked in red. We simulated time series $\{x_t\}_{t \in \{1, \dots, n\}}$ with $n = 51$ data points with $x_t \sim \mathcal{N}_p(0, I_p)$.

et al. [1996] and its implementation in the `qhull` library <http://www.qhull.org/>. The QuickHull algorithm works in any dimension and is reasonably fast for our application up to $p = 5$.

4 On The Detection of a Single Changepoint Online

4.1 From the Functional Description to a Convex Hull

We now apply the results of Section 3 to the problem of detecting a single changepoint described in Section 2.2, to develop an efficient online algorithm. To do this, it is helpful to define a one-to-one mapping P between any changepoint τ and a point in dimension $p + 1$:

$$P(\tau) = \left(\tau, \sum_{t=1}^{\tau} x_t \right). \quad (10)$$

The following theorem, based on Theorem 4 essentially states that the changepoint maximising the likelihood (5) for some value η_1 and η_2 corresponds to a point on a particular convex hull.

Theorem 5. *Assume the log-likelihood, $\ell_{\tau, n}(\eta_1, \eta_2)$ of a change at τ in $\{1, \dots, n-1\}$ can be written as in (5). Then, for any η_1 and $s \leq p$ taking $\hat{\tau} = \hat{\tau}^s(\eta_1)$ or $\hat{\tau}^s(\cdot)$ we have that $P(\hat{\tau})$ is on the convex hull of $\{P(\tau)\}_{\tau \in \{1, \dots, n-1\}}$.*

Remark 1. *This result also extends to other test statistics that maximise the sparse log-likelihood for some s . This includes statistics that threshold the contribution from each component of the time series (see Section I.1 in Supplementary Material).*

Theorem 5 is coherent with the notion of pruning as in the FOCuS algorithm [Romano et al., 2023]. If $P(\tau_0)$ is strictly inside the hull, i.e. not on the boundary of the hull $\{P(\tau)\}_{\tau \in \{1, \dots, n-1\}}$ at time n , then it is inside the hull at any future time $n' \geq n$. Thus, based on Theorem 5, the likelihood associated with the change at time τ_0 will never be optimal after time n .

4.2 Bound on The Number of Changepoint Candidates

From a computational perspective, Theorem 5 is useful only if the set of points on the convex hull is significantly smaller than n . We now use recent results [Kabluhko et al., 2017] to bound the expected number of faces and vertices of the convex hull $\{P(\tau)\}_{\tau \in \{1, \dots, n-1\}}$, assuming that the components of x_τ , x_τ^d (with $d = 1, \dots, p$), are i.i.d. with a continuous distribution. In turn, using Theorem 4, this gives us an upper bound on the expected number of changepoints that can maximise the likelihood function (5) for some value of η_1 and η_2 . This bound will be useful to derive guarantees on the computational complexity of the procedure (see Algorithms 1 and 3).

Theorem 6. *Assuming all x_τ^d (with $d = 1, \dots, p$) are i.i.d. with a continuous distribution, then the expected number of faces (denoted as U_n^p) and vertices (denoted as V_n^p) of the convex hull of $\{P(\tau)\}_{\tau \in \{1, \dots, n-1\}}$ are the following:*

$$\mathbb{E}(U_n^p) = \frac{2p!}{(n-1)!} \left[\begin{matrix} n \\ p+1 \end{matrix} \right], \quad \mathbb{E}(V_n^p) = \frac{2}{(n-1)!} \sum_{l=0}^{\infty} \left[\begin{matrix} n \\ p+1-2l \end{matrix} \right],$$

where $\left[\begin{matrix} n \\ m \end{matrix} \right]$ are the Stirling numbers of the first kind [Adamchik, 1997].

Corollary 1. *We have the following equivalents for the expected numbers of faces U_n^p and vertices V_n^p :*

$$\mathbb{E}(U_n^p) \sim 2 (\log(n))^p, \quad \mathbb{E}(V_n^p) \sim \frac{2}{p!} (\log(n))^p, \quad n \rightarrow \infty.$$

The proof of Corollary 1 follows from Remark 1.4 of Kabluhko et al. [2017]. The theorem and corollary provide an expected upper limit on the number of points, or candidate locations for changepoints, that need to be evaluated to compute the CUSUM likelihood ratio test (5) exactly without resorting to approximations. This limit increases as $\mathcal{O}(\log(n)^p)$ and so will give small bounds on the number of candidate changepoints for small p . We empirically illustrate the validity of Theorem 6 for i.i.d. Gaussian and Poisson data in supplementary material B.5 and F.1.

4.3 MdFOCuS: a Simple Online Algorithm

In this section, we propose an algorithm to compute the GLR statistics at every time step n for a known and unknown pre-change parameter η_1 . In both cases, based on Theorem 5 we only need to consider the changepoints τ such that $P(\tau)$ is on the hull of $\{P(\tau')\}_{\tau' \in \{1, \dots, n-1\}}$.

Let us call \mathcal{T}_n the set of index τ such that $P(\tau) = (\tau, \sum_{t=1}^{\tau} x_t)$ is on the convex hull of all $\{P(\tau)\}_{\tau \in \{1, \dots, n-1\}}$. Restating Theorem 4, the changepoint $\hat{\tau}$ maximising the likelihood

(5) is in \mathcal{T}_n . Hence, at step n , we only need to compute the likelihood (and likelihood ratio statistics) of changepoints τ in \mathcal{T}_n . Furthermore, as already explained after Theorem 5 we can prune all τ that are not in \mathcal{T}_n as they will never be in $\mathcal{T}_{n'}$ for any $n' \geq n$.

Computing the convex hull from scratch at every time step n is inefficient: it requires at least $\mathcal{O}(n)$ operations and leads to an overall complexity at least quadratic in n . Ideally, we would like to update the hull using an efficient online or dynamic convex hull algorithm as the one in Clarkson and Shor [1989]. There exist implementations of such an algorithm in dimensions $p = 2$ [Melkman, 1987] and $p = 3$ [Hert and Schirra, 2023]. However, for simplicity, here we rely on an iterative use of the offline `QuickHull` algorithm [Barber et al., 1996] that also works for larger dimensions and is available in the `geometry` R package [Habel et al., 2023].

In detail, for any $n' > n$ we have $\mathcal{T}_{n'} \subset \mathcal{T}_n \cup \{n, \dots, n' - 1\}$. Therefore if we have already computed \mathcal{T}_n , we only apply `QuickHull` to the points $P(\tau)$ with τ in $\mathcal{T}_n \cup \{n, \dots, n' - 1\}$. A first idea would be to apply the `QuickHull` algorithm at every time step $n, n + 1, \dots$, that is compute \mathcal{T}_n as the hull of all $P(\tau)$ with τ in $\mathcal{T}_{n-1} \cup \{n\}$. In practice, we discovered that running the `QuickHull` algorithm intermittently, rather than at every iteration, resulted in faster run times. Specifically, we maintain a set of linearly increasing indices, denoted as \mathcal{T}'_n , and only periodically execute `QuickHull` to reconstruct the true \mathcal{T}_n . More precisely, to decide when to run `QuickHull`, we update a maximum size variable for \mathcal{T}'_n (denoted `maxSize`). Then, at step $n + 1$:

- if $|\mathcal{T}'_n|$, is smaller than `maxSize` we set \mathcal{T}'_{n+1} to $\mathcal{T}'_n \cup \{n\}$,
- otherwise we compute \mathcal{T}'_{n+1} as the convex hull of all $P(\tau)$ with τ in $\mathcal{T}'_n \cup \{n\}$.

In the latter case we also update `maxSize` to `maxSize = $\lfloor \alpha |\mathcal{T}'_{n+1}| + \beta \rfloor$` , with $\alpha \geq 1$ and $\beta \geq 0$. It is important to note that, in this way, we always retain a few more possible changepoints than necessary: $\mathcal{T}_{n+1} \subseteq \mathcal{T}'_{n+1}$.

If $\beta = 1$ and $\alpha = 1$ we run the `QuickHull` algorithm at every time step. Larger values of α mean we run it less often, but at the cost of having a longer list of indices in \mathcal{T}'_n . We empirically evaluated different values of α with $\beta = 1$, and found $\alpha = 2$ gave good practical performance; see Supplementary Material F.2.

A formal description of our procedure, called MdFOCuS is presented in Algorithm 1. The algorithm covers both known and unknown pre-change parameters η_1 , with the only difference being the calculation of the likelihood (lines 7 and 8). Therefore, the two variants store the same number of candidate changepoints and have the same time and memory complexities. In detail, computing the full likelihood ratio statistics for any particular changepoint has a time complexity of $\mathcal{O}(p)$, and therefore lines 7 and 8 in Algorithm 1 have a complexity of $\mathcal{O}(|\mathcal{T}|p)$. Recovering the maximum has complexity $\mathcal{O}(|\mathcal{T}|)$. Overall, this is $\mathcal{O}(|\mathcal{T}|p)$.

A link to a simple R implementation of Algorithm 1 for a change in the mean of p -dimensional Gaussian signal can be found in the Supplementary Materials. Our code is based on the `convhulln` function implementing the `QuickHull` algorithm in the `geometry` R package, and for $p = 3$ it takes 2 minutes to process $n = 5 \times 10^5$ data points on an Intel(R) Xeon(R) Gold 6252 CPU @ 2.10GHz processor choosing $\alpha = 2$ and $\beta = 1$. As can be seen in Figure 4 (left), such run time is comparable to that of the `ocd` R package [Chen et al., 2022].

Algorithm 1 MdFOCuS algorithm

```
1: Inputs:  $\{x_t\}_{t=1,2,\dots}$   $p$ -variate independent time series;  $thrs$  threshold;  $\eta_1$  pre-change
   parameter (if known);  $maxSize > p + 1$ ,  $\alpha \geq 1$ ,  $\beta \geq 0$ , pruning parameters.
2: Outputs: stopping time  $n$  and maximum likelihood change :  $\hat{\tau}(\cdot)$  or  $\hat{\tau}(\eta_1)$ 
3:  $GLR \leftarrow -\infty$ ,  $\mathcal{T} \leftarrow \emptyset$ ,  $n \leftarrow 1$ 
4: while ( $GLR < thrs$ ) do
5:    $n \leftarrow n + 1$ 
6:    $\mathcal{T} \leftarrow \mathcal{T} \cup \{n - 1\}$ 
7:    $\hat{m} \leftarrow \max_{\tau \in \mathcal{T}} \{\max_{\eta_1, \eta_2} \ell_{\tau, n}(\eta_1, \eta_2)\}$  ▷  $\eta_1$  is fixed if pre-change known
8:    $GLR \leftarrow \hat{m} - \max_{\eta_1, \eta_2} \ell_{n, n}(\eta_1, \eta_2)$  ▷  $\eta_1$  is fixed if pre-change known
9:   if ( $|\mathcal{T}| > maxSize$ ) then
10:     $\mathcal{T} \leftarrow \text{QUICKHULL}(\{P(\tau)\}_{\tau \in \mathcal{T}})$  ▷ Find the indices on the hull of all  $P(\tau)$ 
11:     $maxSize \leftarrow \lfloor \alpha |\mathcal{T}| + \beta \rfloor$ 
12:   end if
13: end while
14: return  $n$  and  $GLR$ 
```

We also implemented Algorithm 1 for a change in the mean of a multi-dimensional Gaussian signal in R/C++ using the `qhull` library. We use the Gaussian distribution as an example of a distribution with continuous density and independent dimensions. To be specific, for p from 1 to 6, we simulated time series $x_{1:n}$, with $x_t \sim \mathcal{N}_p(0, I_p)$ i.i.d. We varied the time series length from $2^{10} + 1 (\approx 10^3)$ to $2^{23} + 1 (\approx 8 \times 10^6)$ and simulated 100 data sets for each length. The average run times as a function of n are presented on the log-scale in Figure 3. As expected, it is faster than our R implementation: for example, for $p = 3$ it processes in 2 minutes for $n = 10^6$ rather than 5×10^5 . The run times for a known or unknown η_1 are almost identical. Finally, we made a simple linear regression to model the logarithm of the run time as a function of $\log(n)$. The estimated slope coefficients are reported in Figure 3 and are all smaller than 1.2.

4.4 A provably quasi-linear online implementation

We showed how Algorithm 1 is exact and empirically fast, but it is non-trivial to derive its worst or expected time complexity as the time at which we run `QuickHull` is stochastic. In Supplementary Material G we propose Algorithm 3 that is closely related but easier to analyse. This algorithm updates the set \mathcal{T} in a deterministic manner on predetermined chunks of the observations. This deterministic choice of chunks allows for a precise quantification of the expected complexity of the algorithm using Corollary 1 and the assumption that the convex hull algorithm is at worst quadratic. To be specific, here are our assumptions.

Assumption 1. *In any dimension $p \geq 1$, there are positive constants c_1 and c_2 for which the expected number of vertices, $\mathbb{E}[V_n^p]$, can be bounded as follows:*

$$\mathbb{E}[V_n^p] \leq c_1 \log(n)^p + c_2.$$

This is true under the conditions of Theorem 6 and Corollary 1. Next, define $Time(n)$ to be the worst-case computational cost of finding the convex hull of n points.

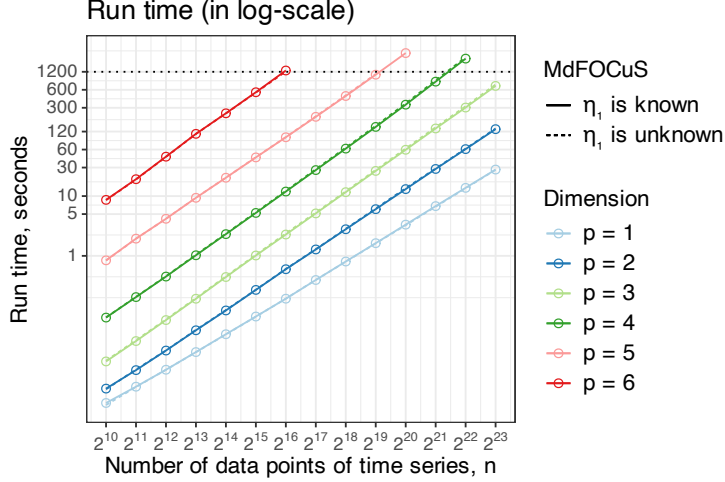


Figure 3: Run times in seconds of MdFOCuS with known (dashed line) and unknown (full line) pre-change parameter η_1 , both with $\alpha = 2$ and $\beta = 1$, in dimension $p = 1, \dots, 6$ for i.i.d Gaussian data. Run times are averaged over 100 data sets. We considered a maximum running time of 20 minutes (horizontal dotted black line) for the algorithms, and thus do not report run times for $p \geq 4$ for large n . The slope of the curves estimated are for known η_1 : ≈ 1.005 ($p = 1$), ≈ 1.116 ($p = 2$), ≈ 1.180 ($p = 3$), ≈ 1.196 ($p = 4$), ≈ 1.143 ($p = 5$) and ≈ 1.202 ($p = 6$); and for unknown η_1 : ≈ 1.006 ($p = 1$), ≈ 1.118 ($p = 2$), ≈ 1.183 ($p = 3$), ≈ 1.202 ($p = 4$), ≈ 1.144 ($p = 5$) and ≈ 1.197 ($p = 6$).

Assumption 2. For our convex hull algorithm there exist two positive constants c_3 and c_4 such that $Time(n) \leq c_3 n^2 + c_4$.

The assumption on the quadratic complexity is true for QuickHull for $p \leq 2$ [Barber et al., 1996] and using the algorithm of Chazelle [1993] it is true for $p \leq 3$.

In essence, Algorithm 3 computes the convex hull using a divide-and-conquer strategy. Out of simplicity, let us consider the offline setting and assume $n - 1$ is a power of 2, that is $n - 1 = 2^{\log_2(n-1)}$. Rather than running the hull algorithm on all points $\{P(\tau)\}_{\tau \in \{1, \dots, n-1\}}$ we first run the algorithm on smaller chunks of size $2^{q_{min}}$: $\tau \in \{2^{q_{min}}j + 1, \dots, 2^{q_{min}}j + 2^{q_{min}}\}$, with q_{min} a constant chosen by the user and j a number smaller than $(n - 1)/2^{q_{min}}$, and then dyadically merge the results. To be specific for each scale q with $q_{min} < q < \log_2(n - 1)$ we get the points on chunk $\{2^{q+1}j + 1, \dots, 2^{q+1}j + 2^{q+1}\}$, by merging the results of the two smaller chunks $\{2^{q+1}j + 1, \dots, 2^{q+1}j + 2^q\}$, and $\{2^{q+1}j + 2^q + 1, \dots, 2^{q+1}j + 2^{q+1}\}$. This merging is computationally efficient because, under Assumption 1, the number of points on the hull of a chunk of size 2^q is expected to be small (of order $(\log(2^q))^p = (q \log(2))^p$).

One difficulty in Algorithm 3 is to make this dyadic or divide-and-conquer merging in an online fashion. To the best of our efforts, this makes the formal description a bit tedious, and we refer the interested reader to the Supplementary Material G and Algorithm 2 and 3 for a precise description. We now state our bound on the expected complexity of Algorithms 2 and 3.

Lemma 1. Under Assumptions 1 and 2, the expected time complexity of Algorithm 2 and 3 is $\mathcal{O}(n \log(n)^{p+1})$.

We empirically study the complexity of Algorithm 3 in Figure 16 of Supplementary Material G, where we see that it is slower than Algorithm 1. It is interesting to compare the bound on the computational cost with that of an oracle algorithm that knows the set of points on the convex hull at each iteration and whose computational cost is only evaluating the test statistic for each point on the hull. This would have a complexity of order $n \log^p(n)$, as $\sum_{t=1}^n \log^p(t) \geq n/2 \log^p(n/2)$. This is just a factor of $\log n$ faster than the bound in Lemma 1.

4.5 Two variant of MdFOCuS

In this subsection, we describe two variants of the algorithm, arising from variations in (i) the test statistic construction and (ii) the convex hull update. These variants are available regardless of whether or not the pre-change parameter is known.

The first variant will allow MdFOCuS to improve on scenarios where only a subset of the coordinates change: out of simplicity in lines 7 and 8 of Algorithm 1 we only consider the likelihood ratio statistics (5) that assumes all coordinates are changing. However, based on Theorem 5, the changepoints maximising the sparse likelihood ratio statistics (2), where only s coordinates are changing, also correspond to points on the hull, and we can compute the test statistics in this case by replacing lines 7 and 8 with the corresponding sparse likelihoods.

To compute all sparse max likelihood ratio statistics we sort the per-dimension ratio statistics (this can be done in $\mathcal{O}(p \log(p))$) and sum these from the largest to the smallest in $\mathcal{O}(p)$ to iteratively recover the best for all sparsity levels s . We then recover the maximum for each sparsity level in $\mathcal{O}(\mathcal{T})$. If we consider all sparsity levels the total complexity is $\mathcal{O}(|\mathcal{T}|p \log(p))$.

In practice, it makes sense to consider a subset of all sparsity levels. In our simulations we consider: $s \in \{2^0, 2^1, 2^2, \dots, 2^{\lfloor \log_2(p) \rfloor}, p\}$. In a similar fashion to the FOCuS approximation, we also consider the sum of the max likelihood ratio statistics for each coordinate. As can be seen in Figure 4, the empirical run time of MdFOCuS with sparse statistics is comparable to that of `ocd` [Chen et al., 2022].

The second variant extends the algorithm to high-dimensional settings, where a full convex hull update is computationally prohibitive. In fact, under the condition of Theorem 6, Algorithm 1 is expected to store $\mathcal{O}(\log^p(n))$ candidates and the $\log^p(n)$ term means that the algorithm is impractical for p larger than 5, as exemplified in Figure 3. In Supplementary Material H, we propose an approximate algorithm by recovering only a subset of the points on the hull. We obtain this subset by considering projections on at most \tilde{p} variates, running the hull algorithm on each projection, and taking the union of the time-points (of the vertices) retained for each projection. For each projection or group of variates, under the condition of Theorem 6, we store $\mathcal{O}(\log^{\tilde{p}}(n))$ candidates. Considering $\mathcal{O}(p)$ such groups we store $\mathcal{O}(p \log^{\tilde{p}}(n))$ candidates, thus reducing the computational complexity.

This heuristic for $\tilde{p} = 2$, implemented in `R`, runs on average in about 100 seconds for $p = 100$ and $n = 10000$. We further explore the run times of this heuristic in Figure 4 and show that its run time is comparable to `ocd`. As shown in Section 4.7 it provides good statistical performance.

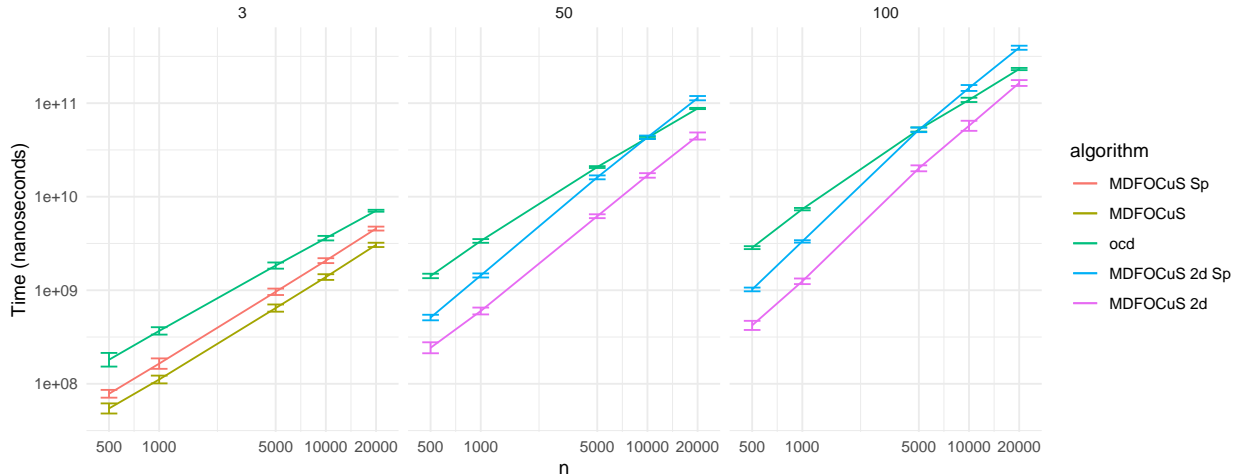


Figure 4: Average run times of MdFOCuS, MdFOCuS with sparse statistics (Sp), and the $2d$ hull approximation and `ocd` over 50 replicates for each scenario, for $p = 3, 50$ and 100 and n varying from 500 to 10000 on an Intel Xeon Gold 6342 (32) @ 2.793GHz.

4.6 Statistical Guarantees

In Supplementary Material I, we provide several statistical guarantees for our procedure considering sparse or dense statistics in the multivariate Gaussian case. Our results also cover test statistics that threshold the contribution from each component. We consider properties of our algorithm if there is no change and then if there is one. In the first scenario, we cover both the pre-change parameter being known or unknown, while in the second, we only consider the pre-change parameter being known. We summarise the main results and their implications here.

We first consider the properties of our algorithm if there is no change. In this case, one may want to control either the false-positive rate, that is, the probability of ever detecting a change, or the average run length, the expected time until we detect a change. Our results give thresholds for both cases, but we will summarise them here just for an average run length of γ . At time n , we define the test statistic assuming a sparsity level s and a candidate change at τ as $S_{\tau,n}^s$. Testing for m different sparsity levels, and with the following threshold for sparsity s

$$c_s(\gamma) = s + 2\zeta + 2\sqrt{s\zeta}, \text{ where } \zeta = 4 \log \gamma + s \log p + \log m + 5 \log 2$$

our MdFOCuS algorithm will have an average run length of at least γ (this follows by applying the argument in Remark 4 to the result of Proposition 8 with $N = 2\gamma$ and $\alpha = 1/2$). In the case where $s = p$ the $s \log(p)$ term in ζ can be omitted.

Next, we consider the power of detecting a change. This can be quantified in terms of the average detection delay, informally the expected time after a change that you would detect it, or bounds on the detection delay, the probability of detecting a change within some time-interval that it occurs. We provide results on both, but will summarise here only the latter. Let the change in mean be specified by the vector δ . For a test at sparsity level s , denote by $\delta^{[s]}$ the vector of length s that consists of the s entries of δ with the largest

absolute value. Finally, let τ^* denote the true changepoint and T^s the time at which we detect a change using the s -sparse statistic. Then from Proposition 9 and Remark 7, and using the threshold $c_s(\gamma)$, we have that with probability at least $(1 - \alpha)$,

$$T^s - \tau^* < \frac{2(c_s(\gamma) - s) + 2\sqrt{s \log(3/\alpha)} - 8 \log(\alpha/3)}{\|\delta^{[s]}\|^2}. \quad (11)$$

We can draw some insights from these results. Excluding $s = p$, first observe that $c_s(\gamma)$ is increasing with s . This means, unsurprisingly, that to minimise the bound on the detection delay $T^s - \tau^*$, we never want to use s greater than the true sparsity of δ , with the notable exception of $s = p$. More generally, it is helpful to consider two different regimes depending on the relative sizes of γ and p . The first is a low-dimensional setting where $\log \gamma$ is much larger than p . In this case, the numerator of the right-hand side of (11) is dominated by the $\log \gamma$ term in $c_s(\gamma)$, and will be approximately $8 \log \gamma / \|\delta^{[s]}\|^2$. In this case, maximising $\|\delta^{[s]}\|^2$ is key to minimising the detection delay, and this can be guaranteed by using the dense test statistic, $s = p$. Any advantage of using smaller s , in the case that some components do not change, will be small.

The other regime is where p is much larger than $\log \gamma$. In this case, using the dense statistics will give a detection delay with leading order (from the right-hand side of Equation 11) that is proportional to $\sqrt{p} / \|\delta\|^2$. By comparison, the s -sparse statistic will have a detection delay with leading order proportional to $(s \log p) / \|\delta^{[s]}\|^2$. If only s components change, and all change by the same amount, then this latter quantity will be lower order in p when $s = o(\sqrt{p})$, as is consistent with other results on high-dimensional change detection [e.g. Chen et al., 2022]. Finally, we can see that the benefit of robustness of performance to the true level of sparsity that comes using $m = O(\log p)$ tests for differing sparsity levels is only a $\log \log p$ increase in the thresholds and hence in the detection delays.

4.7 Empirical statistical performance

In this section, we evaluate the empirical performance of the R implementation of MdFOCuS with the sparse statistics (as in Section 4.5) on synthetic 3, 5, and 100-dimensional time series under the Gaussian change-in-mean setting, with an additional simulation study for a 50-dimensional time series presented in Supplementary Material F.3. We consider two scenarios: pre-change mean known and unknown. For each experiment, we report results aggregated from 300 data sets.

For MdFOCuS for dimension $p = 3$ and 5, we consider sparsity level $s = 1$, the full max-likelihood ratio (either $s = 3$ or $s = 5$ depending on the dimension), and the sum of the max likelihood ratio statistics per dimension as proposed in Romano et al. [2023]. For higher dimensions ($p = 100$ and 50), we use the approximate algorithm with $\tilde{p} = 2$ that analyses $2d$ -projections of the data and set the sparsity levels as in Section 4.5. We compare the performance of MdFOCuS with the high-dimensional online changepoint detection method `ocd` [Chen et al., 2022] and a naive multivariate implementation of FOCuS, obtained by running FOCuS independently for each dimension and summing or taking the maximum of the resulting traces [see Section 6 of Romano et al., 2023] at each iteration. Additionally, as a comparison, for the pre-change mean unknown case, we report results of `ocd` and the pre-

change mean known FOCuS with a plug-in estimate of the pre-change parameter, obtained over a probation (training) period of 250 observations.

Thresholds were selected under a Monte-Carlo simulation to achieve an average run length of 5000 observations. An additional study controlling the false positive rate can be found in Supplementary Material F.3. For a change at $t = 1000$, we evaluate performances for a range of different change magnitudes and sparsity levels. To compare performances across different sparsity regimes, changes in the affected time series were normalised such that the change direction lies in the p -dimensional sphere, i.e., ($\|\eta_1 - \eta_2\|_2^2 = \delta$), where δ is the overall change magnitude and η_1, η_2 are the pre- and post-change means, respectively. Tables 1 to Table 3 show results of the Average Detection Delays (ADDs) for 3, 5, and 100-dimensional time series, respectively.

For all dimensions of time series, in both pre-change parameter known and unknown scenarios, we observe that MdFOCuS generally achieves smaller detection delays in cases where the change affects all the time series and over changes of larger magnitudes. In scenarios with sparsity set to 1, the simple FOCuS aggregation tends to be slightly better. This is expected as if we only have a change in one dimension, both the sparse statistics of FOCuS and MdFOCuS will be the same, but MdFOCuS will have a slightly larger threshold, resulting in a slower delay.

For the pre-change mean known case, over changes of smaller magnitudes, we find MdFOCuS to be relatively close to the best competitor in terms of ADD, while it generally outperforms the other methods for larger changes. Furthermore, MdFOCuS is seen to have consistent performances across different sparsity levels. As `ocd` uses a grid for the possible size of change for each variate, its performance is affected by how close the true change size is to the nearest point on the grid. In particular, its performance deteriorates when the true change is outside the set of grid values. We observe this in its deterioration of performance for low magnitudes (0.125) and large magnitudes (1 or 2), in particular over dimensions $p = 3, 5$.

For the pre-change mean unknown scenario, we observe that MdFOCuS generally outperforms competitor methods for magnitudes larger than 0.250, with the exception of scenarios with a change in a single dimension, as explained above. Moreover, in dimensions $p = 5$ and 100, we can clearly see the advantages of performing the likelihood ratio test for a change when the pre-change mean is unknown over using a plug-in estimate for the pre-change parameter. The only exception occurs in the case of FOCuS, when estimating the pre-change parameter from the training data, for $p = 3$, which outperforms other methods for the smallest size of change. Whilst this might seem counter-intuitive, as the error from the estimation should propagate, in dimension $p = 3$ for a small signal-to-noise ratio, the estimation is good enough to not impair the average run length and increase the thresholds, while benefiting from an easier optimisation (as we see in the pre-change mean known case). However, as we move to higher dimensions $p = 5$ and 100, it is unlikely to obtain a better estimate of the true pre-change parameter simultaneously in all dimensions. This results in larger thresholds to control the desired run length, and therefore in a global loss of power. Of course, having more training observations improves the results, in particular for $p = 3$, however, this still has little to no effect in higher dimensions (see Supplementary Material F.4).

Table 1: Average detection delay with 3-dimensional time series for a change at time $t = 1000$. Pre-change parameter is known on the left, and unknown on the right. Best results per row are highlighted in bold. For the pre-change unknown case FOCuS (est 250) and ocd estimate the pre-change parameter from 250 training samples.

magnitude	sparsity	Pre-change Known			Pre-change Unknown			
		FOCuS	MdFOCuS	ocd	FOCuS (est 250)	FOCuS	MdFOCuS	ocd (est 250)
0.125	1	786.67	806.54	1227.57	1470.76	1644.05	1726.24	1783.41
0.125	2	791.36	817.12	1421.54	1693.06	1770.33	1815.88	1987.04
0.125	3	859.03	886.83	1496.18	1723.76	1806.46	1853.35	2097.23
0.250	1	250.58	255.78	227.18	470.69	340.46	364.50	430.33
0.250	2	253.56	256.76	268.86	556.86	369.36	363.55	516.28
0.250	3	273.92	266.27	300.69	630.94	404.19	395.40	559.66
0.500	1	65.85	66.46	56.46	113.75	69.73	69.36	83.90
0.500	2	71.85	69.93	65.18	132.99	78.42	75.28	96.50
0.500	3	79.21	76.52	74.50	155.61	87.95	84.11	103.97
0.750	1	31.80	32.16	28.95	50.73	32.62	33.22	39.46
0.750	2	34.66	33.31	32.52	61.46	36.15	35.35	43.47
0.750	3	37.19	34.84	35.43	71.75	39.40	36.47	46.40
1.000	1	18.51	19.04	18.87	29.18	19.06	19.53	24.16
1.000	2	20.30	19.53	20.45	34.55	20.94	20.42	25.45
1.000	3	21.68	20.27	21.52	40.03	22.49	20.72	26.23
2.000	1	5.35	5.41	6.40	8.06	5.43	5.53	7.12
2.000	2	5.97	5.72	6.64	9.46	6.13	5.78	7.25
2.000	3	6.51	6.09	6.80	10.62	6.71	6.16	7.41

5 Application to NBA Plus-Minus Data

In this section, we illustrate our methodology to detect a change in the Cleveland Cavaliers (an NBA team) Plus-Minus score from season 2010-11 to 2017-18. This example was proposed in Shin et al. [2022]. We use this example for two reasons. First, it highlights that our computational framework is also applicable to CUSUM Exponential baseline e-detectors proposed in Shin et al. [2022] which in essence are a non parametric generalization of generalized likelihood ratio rules. Second, it illustrates how modelling not only the signal’s mean but also its variance can simplify the calibration of the detection threshold, without necessarily resorting to a non-parametric approach.

We recovered the Plus-Minus score using the `nbastatR` package [Bresler, 2023] available at <https://github.com/abresler/nbastatR>. The Cavaliers Plus-Minus is represented in Figure 5, and is a time series of the difference in score of the Cavaliers and their opponents over successive games. We consider detecting a changepoint in this data online.

As detailed in Shin et al. [2022], it is nontrivial to fit this problem into commonly used parametric sequential changepoint detection procedures for two main reasons. First, it is not easy to choose a parametric model to fit the score. In particular, we would like to take into account that we have integer-valued data, and we expect some form of dependency. Second, assuming we have chosen a model or likelihood function, calibrating the threshold to detect a changepoint is not trivial. A small change in the distribution we use as a reference can

Table 2: Average detection delay with 5-dimensional time series for a change at time $t = 1000$. Pre-change parameter is known on the left, and unknown on the right. Best results per row are highlighted in bold. For the pre-change unknown case FOCuS (est 250) and ocd estimate the pre-change parameter from 250 training samples.

magnitude	sparsity	Pre-change Known			Pre-change Unknown			
		FOCuS	MdFOCuS	ocd	FOCuS (est 250)	FOCuS	MdFOCuS	ocd (est 250)
0.125	1	833.11	866.74	911.17	2219.97	1718.76	1802.03	2458.66
0.125	2	892.82	918.78	1106.68	2221.24	1874.47	2049.54	2441.70
0.125	3	925.08	940.54	1101.38	2255.65	1924.89	2036.49	2493.92
0.125	4	835.44	836.87	1059.06	2102.15	1825.65	1881.13	2296.26
0.125	5	953.85	948.59	1297.37	2228.96	2005.88	2062.98	2448.01
0.250	1	259.75	267.12	229.64	871.35	360.65	368.47	1064.11
0.250	2	281.77	279.88	253.79	963.88	433.69	450.35	1084.21
0.250	3	297.41	289.83	287.10	1004.43	456.72	467.69	1077.31
0.250	4	260.23	242.46	265.40	918.63	413.22	382.42	852.33
0.250	5	304.13	288.07	309.16	1023.24	504.75	495.38	1000.05
0.500	1	72.98	73.81	64.74	206.83	80.54	80.69	247.08
0.500	2	84.75	80.83	73.93	243.50	95.86	91.35	253.56
0.500	3	91.31	84.41	83.54	267.82	103.57	96.62	252.69
0.500	4	80.89	71.59	75.94	250.83	94.23	81.13	199.82
0.500	5	95.41	86.77	89.48	293.72	110.49	100.25	235.87
0.750	1	33.44	34.02	32.98	91.82	34.46	35.00	108.72
0.750	2	39.21	37.79	36.22	113.10	40.34	39.06	113.74
0.750	3	41.29	38.16	38.61	124.88	44.27	41.49	110.91
0.750	4	37.03	33.10	34.71	116.62	41.61	35.94	87.09
0.750	5	45.65	40.26	42.24	137.55	50.88	44.03	104.84
1.000	1	19.63	19.84	21.37	51.75	20.02	20.30	62.33
1.000	2	22.88	21.86	22.88	63.86	23.55	22.49	62.99
1.000	3	24.67	22.83	23.65	71.35	25.38	23.47	62.24
1.000	4	22.45	19.29	20.32	67.41	23.76	20.20	49.88
1.000	5	27.18	23.63	25.07	81.02	28.62	24.79	61.01
2.000	1	5.79	5.84	7.25	13.40	5.73	5.82	15.78
2.000	2	6.88	6.58	7.47	16.57	6.86	6.53	15.66
2.000	3	7.21	6.55	7.33	18.62	7.29	6.72	15.74
2.000	4	6.64	5.72	6.10	17.92	6.92	5.90	12.99
2.000	5	7.91	6.87	7.40	21.30	8.24	7.08	15.55

substantially change the threshold and as a consequence increase the detection time or lead to false detections. E-detectors [Shin et al., 2022], are a non-parametric solution to these two problems.

5.1 Convex hull for CUSUM e-detectors

Following Equations (27) and (41) of Shin et al. [2022] we can write their update of the e-detector CUSUM statistics for a given λ as

$$M_n^{CU}(\lambda) = \exp(\lambda s(x_n) - \psi(\lambda)v(x_n)) \max\{M_{n-1}^{CU}(\lambda), 1\},$$

Table 3: Average detection delay with 100-dimensional time series for a change at time $t = 1000$. Pre-change parameter is known on the left, and unknown on the right. Best results per row are highlighted in bold. For the pre-change unknown case FOCuS (est 250) and ocd estimate the pre-change parameter from 250 training samples.

magnitude	sparsity	Pre-change Known			Pre-change Unknown			
		FOCuS	MdFOCuS	ocd	FOCuS (est 250)	FOCuS	MdFOCuS	ocd (est 250)
0.125	1	1417.15	1391.54	1171.63	3459.08	2708.45	2704.65	3546.43
0.125	5	1881.10	1810.57	1627.00	3497.94	2859.51	2872.20	3595.24
0.125	10	2084.84	1978.85	1940.41	3501.48	2846.45	2874.17	3595.46
0.125	50	2252.48	2289.56	2386.98	3494.67	2888.46	2881.59	3591.96
0.125	100	2323.59	2338.00	2431.51	3507.66	2859.11	2887.60	3599.24
0.250	1	389.11	380.09	335.95	2659.50	730.54	720.45	2841.37
0.250	5	641.18	555.57	505.39	3054.36	1520.80	1451.53	3232.02
0.250	10	789.27	673.15	595.10	3178.29	1879.64	1692.20	3334.21
0.250	50	1057.30	895.53	827.30	3323.17	2353.01	2309.73	3453.27
0.250	100	1080.26	916.64	891.09	3346.50	2341.24	2414.38	3476.58
0.500	1	105.79	107.89	104.79	721.53	118.84	121.50	859.71
0.500	5	169.93	147.36	139.23	1297.63	214.14	185.07	1449.56
0.500	10	232.04	176.44	170.03	1653.97	296.51	217.84	1850.22
0.500	50	357.90	248.41	239.08	2480.88	578.17	348.83	2719.69
0.500	100	372.34	254.51	244.07	2611.86	679.19	365.79	2841.33
0.750	1	47.78	48.67	57.56	310.89	50.08	50.68	461.51
0.750	5	75.34	66.80	73.47	580.05	85.34	73.90	715.73
0.750	10	104.45	80.81	84.16	798.60	117.25	88.30	925.56
0.750	50	184.09	116.47	114.29	1626.21	239.73	133.60	1836.28
0.750	100	193.77	120.24	115.21	1823.30	279.42	137.98	2074.96
1.000	1	27.12	27.55	38.67	173.04	27.76	28.41	317.49
1.000	5	43.72	39.02	46.07	325.28	46.44	41.45	476.20
1.000	10	60.36	47.40	50.77	458.62	63.85	49.35	599.74
1.000	50	109.11	67.33	66.02	1074.41	135.79	73.06	1218.93
1.000	100	116.60	69.23	67.59	1288.45	157.47	75.55	1466.28
2.000	1	7.58	7.65	12.93	43.03	7.53	7.73	142.00
2.000	5	12.92	11.12	13.80	82.41	12.95	11.33	203.48
2.000	10	16.46	13.16	14.80	117.67	16.30	13.48	250.44
2.000	50	31.85	18.37	18.08	315.56	34.85	18.70	451.59
2.000	100	34.28	18.97	18.34	422.46	41.93	19.37	493.39

where λ is in a subset of \mathbb{R} , s and v are real-valued functions, and ψ is a finite and strictly convex function. Taking logs and considering all possible changepoints prior to n we recover with induction that

$$\log(M_n^{CU}(\lambda)) = \max_{\tau < n} \left\{ \sum_{t=\tau+1}^n (\lambda s(x_t) - \psi(\lambda)v(x_t)) \right\}.$$

By subtracting $\sum_{t=1}^n (s(x_t)\lambda - \psi(\lambda)v(x_t))$ in the previous bracket, we do not change the maximiser, and we recover our functional pruning framework of Equation (8) with $a_\tau = \sum_{t=1}^\tau v(x_t)$, and $2b_\tau = \sum_{t=1}^\tau s(x_t)$. Applying Theorem 4 we get that the changepoint optimising the e-detector CUSUM score for any λ value corresponds to a vertex on the

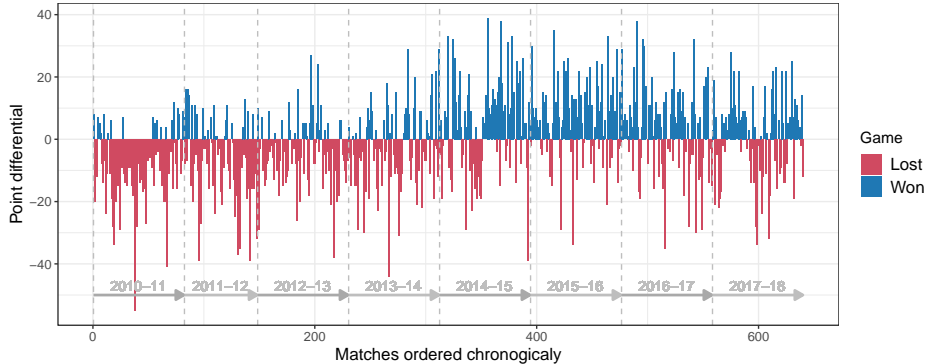


Figure 5: Plus-Minus score of the Cavaliers from season 2010-11 to season 2017-18 as a bar plot. Losses are in dark red and wins are in dark blue. Ends of seasons are represented with vertical dashed lines and seasons are shown on the bottom with grey arrows.

convex hull of

$$\left(\sum_{t=1}^{\tau} v(x_t), \frac{1}{2} \sum_{t=1}^{\tau} s(x_t) \right)_{\tau < n}. \quad (12)$$

As argued in Shin et al. [2022] it makes sense to consider a mixture of e-detectors, that is different λ values. For computational reasons [Shin et al., 2022] considered a finite number of values, chosen using their `computeBaseLine` function.

We will now compare the baseline numbers of two e-detectors for Plus-Minus score to the number of points on the hull of (12). Shin et al. [2022] considered two e-detector models. In the first, which we call `Winning rate`, they model the winning rate and consider $v(x_t) = 1$ and $s(x_t) = \mathbb{1}_{x_t > 0} - p_0$, where $\mathbb{1}$ is the indicator function and p_0 is taken to be 0.49 in the numerical application. With `computeBaseLine` they selected 69 λ values. In their second e-detector model, which we call `Plus-Minus`, they analyse the Plus-Minus score more directly. The score is first normalized between 0 and 1 as $x'_t = (x_t + 80)/160$. Then they define $s(x') = (x'/m - 1)$ and $v(x) = (x'/m - 1)^2$, where m is chosen to be 0.494 in the numerical application. With `computeBaseLine` they selected 190 λ values. For both e-detectors we computed the number of points in the convex hull for n between 10 and $n = 640$ (the last match of season 2017-18) and obtained for `Winning rate` at most 16 and for `Plus-Minus` at most 18 points. Therefore out of the, respectively, 69 and 190 candidates suggested by `computeBaseLine` many are redundant as they correspond to the same changepoint.

5.2 A parametric approach to the Plus-Minus score

Considering a change in the mean of a Gaussian model to fit the Plus-Minus score of the Cavaliers does not take into account the discrete nature of the data and possible dependencies. It is also not clear how one could get a valid estimation of the pre-changepoint parameter. Finally, as argued in Shin et al. [2022] calibrating the threshold to detect a changepoint is not trivial. As a robust parametric solution to these problems, we consider a change in the mean and variance of a univariate Gaussian signal with unknown pre-changepoint parameters.

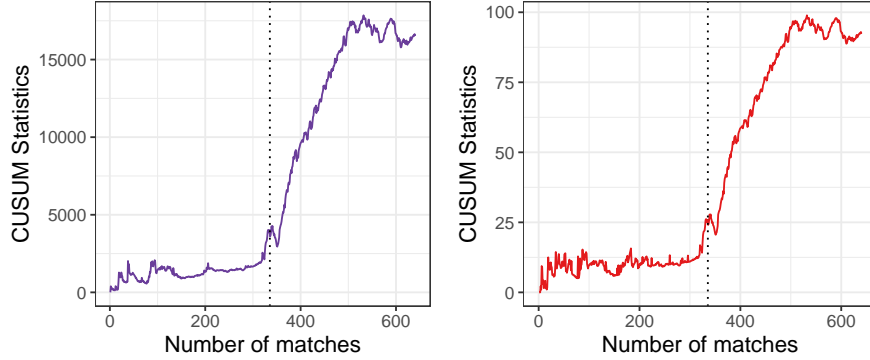


Figure 6: CUSUM statistics for the mean model (left) for the mean and variance model (right). The dotted line corresponds to the beginning of season 2014-15 and match number 312.

For a change in mean and variance using our convex hull framework (8) we need to keep track of the vertices on the hull of a 3-dimensional set of points

$$\left(\tau, \sum_{t=1}^{\tau} x_t, \sum_{t=1}^{\tau} x_t^2 \right)_{\tau < n} . \quad (13)$$

Interestingly, this mean and variance model is invariant to shift and scaling. Based on that, we see that all the points on the convex hull of the Plus-Minus e-detector are on the hull of the change in mean and variance model.

As the data is discrete, two (or more) consecutive scores may be exactly equal. For segments containing equal scores, the estimated variance would be 0, and the likelihood would blow up to infinity. To get around this problem we considered a minimum value for the variance, which we set to 1 (chosen as substantially below the variance seen for plus-minus statistics for NBA teams).

In Figure 6 we represent the CUSUM statistics for the change in mean and change in mean and variance model. Although the scales are quite different, the two statistics have very similar trends and importantly both seem to increase around season 2013-14 (starting at match number 312 represented by a vertical dotted line). Although both models reconstruct the same changepoint, we will see in the next subsection that the mean-variance model shows less variability in terms of detection delay, achieving faster detections once a threshold is set to achieve a fixed run length.

Interestingly, at any time-point after 320 (8th match of season 2014-15) the maximum likelihood changepoint is always between matches 279 and 280 (5th and 7th of February 2014) for both models. This is well before the beginning of season 2014-15 and the comeback of LeBron James. However, this matches the arrival of David Griffin as general manager on the 6th of February [Wikipedia, 2023].

5.3 Simulating NBA Plus-Minus scores without changepoint

Based on Figure 6 it is clear that for a particular range of the threshold both the mean and mean and variance model with unknown pre-changepoint parameter can detect a change-

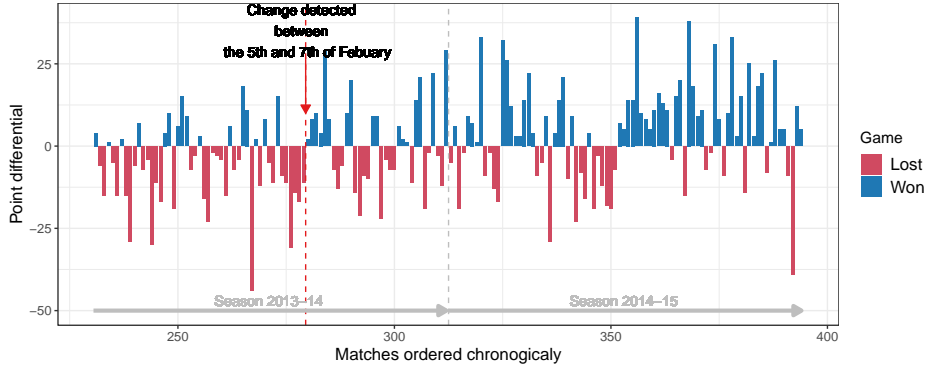


Figure 7: Plus-Minus score of the Cavaliers from seasons 2013-14 to 2014-15 as a bar plot. Losses are in dark red and wins are in dark blue. The ends of seasons are represented with vertical dashed lines (grey) and seasons are shown on the bottom with grey arrows.

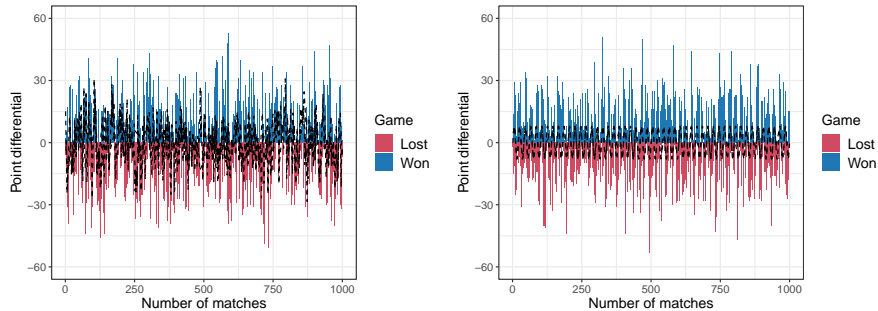


Figure 8: Two Plus-Minus score simulation examples based on the Negative Binomial model with a mean of 115 and scale parameter of 50 using two dependency scenarios: an AR(1) model with AR parameter 0.6 (left) and using sine waves with a period of 20 matches (right).

point after the beginning of season 2014-15. To calibrate this threshold one typically needs a simulation model. Below we consider different choices of simulation model to see how sensitive the threshold is to this choice for both models. In all cases we will set the CUSUM threshold such that under our null simulation over 1000 matches we would detect a change only in 5% of the cases.

The simulation models we considered are: (i) the difference of two independent Poisson random variables; (ii) the difference of two negative binomial random variables; (iii) a uniform distribution on $\{-80, \dots, 80\}$ [as suggested in Shin et al., 2022]; (iv) an independent resampling of past games. For (i) and (ii) we consider a range of parameters, with the mean of the random variables set to be 95, 105 or 115; and with the negative-binomial scale parameter set to 1 or 2. For (iv) we considered either sampling past matches of the Cavaliers or of NBA teams in general, from seasons 1999/2000 to 2009/10. Finally we also considered version of the scenarios in (i) and (ii) where we introduced temporal dependencies by adding to the mean a time-varying function either simulated from an AR(1) model with auto-correlation of 0.6 or using a sin function.

Figure 9 shows the various thresholds we get for our two models, and the corresponding

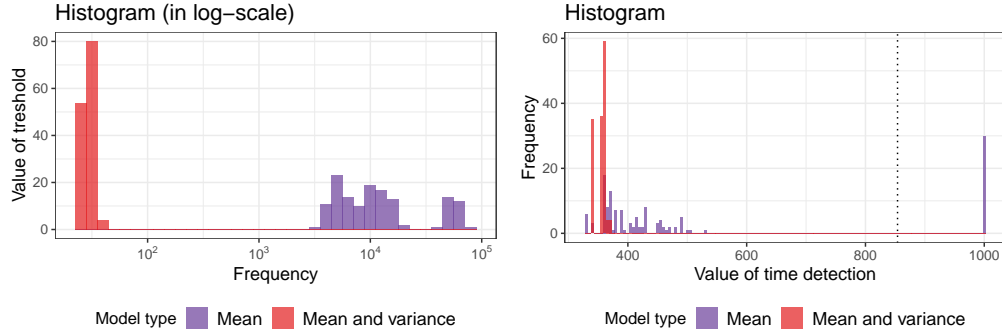


Figure 9: Threshold (left) and detection time (right) obtained for the mean model and the mean and variance model.

detection times. The threshold is much more variable for the change in mean model and this translates to a much more variable detection time. To be specific for the mean model, the change is detected at the earliest at match 330 (the 5th of December 2014), but in 21.7% of the cases the threshold is so high that the changepoint is never detected (reported in the histogram as a detection at 1000). For the mean and variance model, the change is always detected at the earliest at match 339 (the 23rd of December 2014) and at the latest at match 368 (the 20th of February 2015). In fact in 94.2% of the simulation models the change is detected before with the mean and variance model.

6 Discussion

In this paper, we establish a connection between the detection of a single changepoint in p -dimensional data streams and a convex hull problem in dimension $p + 1$. Based on this, we derive a simple yet efficient algorithm, MdFOCuS. This algorithm finds a set of time-points that contain the points associated with all vertices of a convex hull, and that we show contains all possible times that can maximise the likelihood-ratio statistic for a change. The method is general in that it can be used for a wide-range of models from the exponential family, including multivariate data where different streams are modelled by different distributions. It can also deal with the pre-change parameter being known or unknown, and covers tests where we allow only a subset of components of a multivariate data stream change. For all these varieties, the only difference is the part of the algorithm which maximises the function associated with each time-point we have stored. We also showed that it can be used to speed up the calculation of e-detectors. MdFOCuS is efficient for $p \leq 5$. For larger p we provide an approximation storing only $\mathcal{O}(p \log^{\tilde{p}}(n))$ vertices of the convex hull where $\tilde{p} \leq p$.

Improvements to the computational complexity of the procedure could be made to allow the procedure to scale to higher dimensions and longer sequences. For example, a sequential update of the boundary of the convex hull of our points, to improve on the complexity of QuickHull. Recently, Ward et al. [2024] offered an approach to speed-up the maximisation step. This aims to recycle calculations to give a bound on the test statistic that is much more efficient to calculate. Whilst this idea can directly be applied in the multivariate settings we consider, the bounds are too loose to give any noticeable speed-up. A less conservative

bound could be the object of future study.

More generally, the ideas in this paper which show a connection between changepoint detection and convex hull (or half-space intersection) problems sheds light on the geometric nature of the changepoint detection problem and is a promising line for future research.

References

- V. S. Adamchik. On Stirling numbers and Euler sums. *Journal of Computational and Applied Mathematics*, 79:119–130, 1997.
- E. Andreou and E. Ghysels. Detecting multiple breaks in financial market volatility dynamics. *Journal of Applied Econometrics*, 17(5):579–600, 2002.
- A. Aue, L. Horváth, M. Hušková, and P. Kokoszka. Change-point monitoring in linear models. *The Econometrics Journal*, 9(3):373–403, 2006.
- I. E. Auger and C. E. Lawrence. Algorithms for the optimal identification of segment neighborhoods. *Bulletin of Mathematical Biology*, 51(1):39–54, Jan 1989. doi: 10.1007/BF02458835.
- D. Avis and D. Bremner. How good are convex hull algorithms? In *Proceedings of the Eleventh Annual Symposium on Computational Geometry*, pages 20–28, 1995.
- J. Bai and P. Perron. Computation and analysis of multiple structural change models. *Journal of Applied Econometrics*, 18(1):1–22, 2003. doi: <https://doi.org/10.1002/jae.659>.
- C. B. Barber, D. P. Dobkin, and H. Huhdanpaa. The quickhull algorithm for convex hulls. *ACM Trans. Math. Softw.*, 22(4):469–483, dec 1996. doi: 10.1145/235815.235821.
- M. Bosc, F. Heitz, J.-P. Armspach, I. J. Namer, D. Gounot, and L. Rumbach. Automatic change detection in multimodal serial MRI: application to multiple sclerosis lesion evolution. *NeuroImage*, 20:643–656, 2003.
- A. Bresler. *nbastatR: R’s interface to NBA data*, 2023. URL <https://github.com/abresler/nbastatR>. R package version 0.1.152.
- A. Brøndsted. *An introduction to convex polytopes, by A. Brøndsted. Pp 160. DM69. 1983. ISBN3-540-90722-X (Springer-Verlag)*. Springer New York, NY, 1983. doi: <https://doi.org/10.1007/978-1-4612-1148-8>.
- D. R. Chand and S. S. Kapur. An algorithm for convex polytopes. *J. ACM*, 17:78–86, 1970.
- B. Chazelle. An optimal convex hull algorithm in any fixed dimension. *Discrete & Computational Geometry*, 10(4):377–409, 1993. doi: 10.1007/BF02573985.
- Y. Chen, T. Wang, and R. J. Samworth. High-dimensional, multiscale online changepoint detection. *Journal of the Royal Statistical Society Series B: Statistical Methodology*, 84(1): 234–266, 2022.

- K. L. Clarkson and P. W. Shor. Applications of random sampling in computational geometry, ii. *Discrete & Computational Geometry*, 4(5):387–421, 1989. doi: 10.1007/BF02187740.
- J.-F. Ducré-Robitaille, L. A. Vincent, and G. Boulet. Comparison of techniques for detection of discontinuities in temperature series. *International Journal of Climatology*, 23, 2003.
- P. Eiauer and P. Hackl. The use of mosums for quality control. *Technometrics*, 20(4): 431–436, 1978.
- P. Fryzlewicz. Wild binary segmentation for multiple change-point detection. *The Annals of Statistics*, 42(6), dec 2014. doi: 10.1214/14-aos1245.
- E. Galceran, A. Cunningham, R. Eustice, and E. Olson. Multipolicy decision-making for autonomous driving via changepoint-based behavior prediction: Theory and experiment. *Autonomous Robots*, 41, 08 2017. doi: 10.1007/s10514-017-9619-z.
- D. Garreau and S. Arlot. Consistent change-point detection with kernels, 2017.
- K. Habel, R. Grasman, R. B. Gramacy, P. Mozharovskiy, and D. C. Sterratt. *geometry: Mesh Generation and Surface Tessellation*, 2023. URL <https://CRAN.R-project.org/package=geometry>. R package version 0.4.7.
- S. Hert and S. Schirra. 3D convex hulls. In *CGAL User and Reference Manual*. CGAL Editorial Board, 5.6 edition, 2023. URL <https://doc.cgal.org/5.6/Manual/packages.html#PkgConvexHull3>.
- B. Jackson, J. D. Scargle, D. Barnes, S. Arabhi, A. Alt, P. Gioumouisis, E. Gwin, P. Sangtrakulcharoen, L. Tan, and T. T. Tsai. An algorithm for optimal partitioning of data on an interval. *IEEE Signal Processing Letters*, 12(2):105–108, 2005.
- S. Jewell, P. Fearnhead, and D. Witten. Testing for a change in mean after changepoint detection. *Journal of the Royal Statistical Society, Series B*, 84(4):1082–1104, 2022.
- Z. Kabluchko, V. Vysotsky, and D. Zaporozhets. Convex hulls of random walks: Expected number of faces and face probabilities., 2017.
- B. Kenwright. Convex hulls: Surface mapping onto a sphere, 2023.
- R. Killick, P. Fearnhead, and I. A. Eckley. Optimal detection of changepoints with a linear computational cost. *Journal of the American Statistical Association*, 107(500):1590–1598, 2012.
- W. R. Lai, M. D. Johnson, R. Kucherlapati, and P. J. Park. Comparative analysis of algorithms for identifying amplifications and deletions in array CGH data. *Bioinformatics*, 21(19):3763–3770, 2005.
- B. Laurent and P. Massart. Adaptive estimation of a quadratic functional by model selection. *Annals of Statistics*, pages 1302–1338, 2000.

- M. Lavielle and E. Moulines. Least-squares estimation of an unknown number of shifts in a time series. *Journal of Time Series Analysis*, 21(1):33–59, 2000.
- E. Lebarbier. Detecting multiple change-points in the mean of Gaussian process by model selection. *Signal Processing*, 85:717–736, 04 2005. doi: 10.1016/j.sigpro.2004.11.012.
- A. Liehrmann, G. Rigaiil, and T. D. Hocking. Increased peak detection accuracy in over-dispersed ChIP-seq data with supervised segmentation models. *BMC Bioinformatics*, 22(1):1–18, 2021.
- R. Maidstone, T. Hocking, G. Rigaiil, and P. Fearnhead. On optimal multiple changepoint algorithms for large data. *Statistics and Computing*, 27(2):519–533, Mar 2017.
- A. Meier, C. Kirch, and H. Cho. mosum: A package for moving sums in change-point analysis. *Journal of Statistical Software*, 97:1–42, 2021.
- A. Melkman. On-line construction of the convex hull of a simple polyline. *Information Processing Letters*, 25(1):11–12, Apr. 1987. doi: 10.1016/0020-0190(87)90086-X.
- R. Miller and Q. Stout. Efficient parallel convex hull algorithms. *IEEE Transactions on Computers*, 37(12):1605–1618, 1988. doi: 10.1109/12.9737.
- A. Olshen, E. Venkatraman, R. Lucito, and M. Wigler. Circular binary segmentation for the analysis of array-based dna copy number data. *Biostatistics (Oxford, England)*, 5:557–72, 11 2004. doi: 10.1093/biostatistics/kxh008.
- J. O’Rourke. *Convex Hulls in Three Dimensions.*, page 101–154. Cambridge University Press, 2 edition, 1998. doi: 10.1017/CBO9780511804120.005.
- E. S. Page. Continuous inspection schemes. *Biometrika*, 41(1/2):100–115, 1954.
- F. Picard, S. Robin, M. Lavielle, C. Vaisse, and J.-J. Daudin. A statistical approach for array CGH data analysis. *BMC Bioinformatics*, 6:np, 2005. doi: 10.1186/1471-2105-6-27.
- L. Pishchagina, G. Rigaiil, and V. Runge. Geometric-based pruning rules for change point detection in multiple independent time series. *arXiv preprint arXiv:2306.09555*, 2023.
- F. P. Preparata and S. J. Hong. Convex hulls of finite sets of points in two and three dimensions. *Communications of the ACM*, 20(2):87–93, feb 1977. doi: 10.1145/359423.359430.
- F. P. Preparata and D. E. Muller. Finding the intersection of n half-spaces in time $o(n \log n)$. *Theoretical Computer Science*, 8(1):45–55, 1979.
- R. Radke, S. Andra, O. Al-Kofahi, and B. Roysam. Image change detection algorithms: a systematic survey. *IEEE Transactions on Image Processing*, 14(3):294–307, 2005. doi: 10.1109/TIP.2004.838698.
- A. Ranganathan. Pliss: Labeling places using online changepoint detection. *Auton. Robots*, 32(4):351–368, may 2012. doi: 10.1007/s10514-012-9273-4.

- J. Reeves, J. Chen, X. L. Wang, R. Lund, and Q. Q. Lu. A review and comparison of changepoint detection techniques for climate data. *Journal of Applied Meteorology and Climatology*, 46(6):900 – 915, dec 2007. doi: 10.1175/JAM2493.1.
- G. Rigaiil. A pruned dynamic programming algorithm to recover the best segmentations with 1 to k_{max} change-points. *Journal de la Société Française de Statistique*, 156(4): 180–205, 2015.
- G. Romano, I. A. Eckley, P. Fearnhead, and G. Rigaiil. Fast online changepoint detection via functional pruning CUSUM statistics. *Journal of Machine Learning Research*, 24(81): 1–36, 2023.
- V. Runge. Is a finite intersection of balls covered by a finite union of balls in Euclidean spaces? *Journal of Optimization Theory and Applications*, 187(2):431–447, 2020.
- D. Rybach, C. Gollan, R. Schluter, and H. Ney. Audio segmentation for speech recognition using segment features. In *2009 IEEE International Conference on Acoustics, Speech and Signal Processing*, pages 4197–4200, 2009. doi: 10.1109/ICASSP.2009.4960554.
- A. J. Scott and M. Knott. A cluster analysis method for grouping means in the analysis of variance. *Biometrics*, pages 507–512, 1974.
- R. Seidel. Convex hull computations. In *Handbook of discrete and computational geometry*, pages 687–703. Chapman and Hall/CRC, 2017.
- J. Shin, A. Ramdas, and A. Rinaldo. E-detectors: a nonparametric framework for sequential change detection. *arXiv preprint arXiv:2203.03532*, 2022.
- D. Siegmund and E. Venkatraman. Using the generalized likelihood ratio statistic for sequential detection of a change-point. *The Annals of Statistics*, pages 255–271, 1995.
- M. Staudacher, S. Telser, A. Amann, H. Hinterhuber, and M. Ritsch-Martel. A new method for change-point detection developed for on-line analysis of the heart beat variability during sleep. *Physica A-statistical Mechanics and Its Applications*, 349:582–596, 2005.
- H. Wang and Y. Xie. Sequential change-point detection: Computation versus statistical performance. *Wiley Interdisciplinary Reviews: Computational Statistics*, page e1628, 2022.
- K. Ward, G. Dilillo, I. Eckley, and P. Fearnhead. Poisson-focus: An efficient online method for detecting count bursts with application to gamma ray burst detection. *Journal of the American Statistical Association*, pages 1–13, 2023.
- K. Ward, G. Romano, I. Eckley, and P. Fearnhead. A constant-per-iteration likelihood ratio test for online changepoint detection for exponential family models. *Statistics and Computing*, 34(3):99, 2024.
- Wikipedia. David griffin — Wikipedia, 2023. URL [https://en.wikipedia.org/wiki/David_Griffin_\(basketball\)](https://en.wikipedia.org/wiki/David_Griffin_(basketball)). [Online; accessed 27-Oct-2023].

- Y.-C. Yao. Estimation of a noisy discrete-time step function: Bayes and empirical Bayes approaches. *The Annals of Statistics*, 12(4):1434–1447, 12 1984. doi: 10.1214/aos/1176346802.
- Y. Yu, O. H. Madrid Padilla, D. Wang, and A. Rinaldo. A note on online change point detection. *Sequential Analysis*, 42(4):438–471, 2023.

Supplementary Material for ‘Multivariate Maximum Likelihood Changepoint Detection via Half-Space Intersection and Convex Hull’

A Overview of Code

The implementation of the MdFOCuS algorithm, the Plus-Minus score data, the computer code for the simulation study, and the applications discussed in this article can be found in the following GitHub repositories:

- <https://github.com/guillemr/Focused/tree/main> is a link to the R implementation of the MdFOCuS and code for simulation studies.
- <https://github.com/lpishchagina/focus> is a link to the R/C++ implementation of the MdFOCuS algorithm.
- https://github.com/grosed/changepoint_online is a link to the Python implementation of the MdFOCuS algorithm.
- <https://github.com/lpishchagina/dyadicMdFOCuS> is a link to the R/C++ implementation of the MdFOCuS algorithm with dyadic update. It is a different repository from the MdFOCuS algorithm because the dyadic version is interesting mostly from a theoretical perspective to bound the expected complexity but empirically much slower than MdFOCuS;
- <https://github.com/abresler/nbastatR> is the R package Bresler [2023] we used to recover the Plus-Minus score data.

B Proofs

B.1 Proof of Theorem 2

Consider that τ is in $\mathcal{G}_{\mathcal{T}}$. By definition, there exists $(\lambda_0, \mu_0) \in \text{Im}(A) \times \mathcal{D}_A = \mathbb{R}^+ \times \mathbb{R}^p$ such that for all $\tau' \neq \tau$ in \mathcal{T} we have: $g_{\tau}(\lambda_0, \mu_0) > g_{\tau'}(\lambda_0, \mu_0)$. Multiplying by $\alpha > 0$ we get by linearity

$$g_{\tau}(\alpha\lambda_0, \alpha\mu_0) = \alpha g_{\tau}(\lambda_0, \mu_0) > \alpha g_{\tau'}(\lambda_0, \mu_0) = g_{\tau'}(\alpha\lambda_0, \alpha\mu_0).$$

Therefore, the optimality of index τ is true on the half-line $\{\alpha(\lambda_0, \mu_0), \alpha > 0\}$. Note that we can exclude the cases $\|\mu_0\| = 0$ or $\lambda_0 = 0$ as, by a continuity argument, the optimal set for index τ in $\mathcal{G}_{\mathcal{T}}$ (if non empty) is an open set.

We now search for $\alpha_0 \in (0, +\infty)$ such that for any index $\tau'' \in \mathcal{T}$, $g_{\tau''}(\alpha_0\lambda_0, \alpha_0\mu_0) = f_{\tau''}(\alpha_0\mu_0)$. If such α_0 exists, we have

$$a_{\tau''}\alpha_0\lambda_0 - 2\langle\alpha_0\mu_0, b_{\tau''}\rangle = a_{\tau''}\|\alpha_0\mu_0\|^q - 2\langle\alpha_0\mu_0, b_{\tau''}\rangle,$$

leading to solution $\alpha_0 = \frac{\lambda_0^{\frac{1}{q-1}}}{\|\mu_0\|_{\frac{q}{q-1}}}$. α_0 is well defined as we excluded $\|\mu_0\| = 0$ and $\lambda_0 = 0$. Further, note that the result is still true for $a_{\tau} = 0$ or $a_{\tau'} = 0$.

B.2 Proof of Theorem 4

Consider any τ in $\mathcal{G}_{\mathcal{T}}$. Using Theorem 3 we have that $h_{\tau}(\kappa, \lambda, \mu) = 0$ and for all $\tau' \neq \tau$ $h_{\tau'}(\kappa, \lambda, \mu) < 0$. It can not be that $\lambda = 0$ and $\mu = 0$ as in that case $h_{\tau}(\kappa, 0, 0) = 0$ and then $\kappa = 0$, and $h_{\tau'}(\kappa, 0, 0) = 0$ contradicting $h_{\tau'}(\kappa, \lambda, \mu) < 0$.

Now we have the following equivalence:

1. $\exists \kappa, \lambda, \mu$, with $(\lambda, \mu) \neq 0$ such that $h_{\tau}(\kappa, \lambda, \mu) = 0$ and $\forall \tau' \neq \tau \quad h_{\tau'}(\kappa, \lambda, \mu) < 0$.
2. $\exists \kappa, \lambda, \mu$, with $(\lambda, \mu) \neq 0$ such that $\langle (a_{\tau}, b_{\tau}), (\lambda, -2\mu) \rangle = \kappa$ and $\forall \tau' \neq \tau \quad \langle (a_{\tau'}, b_{\tau'}), (\lambda, -2\mu) \rangle < \kappa$.
3. (a_{τ}, b_{τ}) is on the convex hull $\{(a_{\tau}, b_{\tau})\}_{\tau \in \mathcal{T}}$.

To go from point 2 to point 3 we note that a point is a part of the convex hull if there is a hyperplane (defined by a non-zero vector and a constant) going through this point and such that all other points are strictly on one side of the hyperplane.

B.3 Proof of Theorem 5

First consider the case $s = p$. Starting from (5), we get to (7) as described in Section 2.2 and we recover our functional pruning problem of equation (9) as described in Section 3.1, taking $\mathcal{T} = \{1, \dots, n-1\}$, $a_{\tau} = \tau$ and $b_{\tau} = \sum_{t=1}^{\tau} x_t$. Thus applying Theorem 4, and then Theorem 1 we get the desired result for $\hat{\tau}(\eta_1)$.

The index maximising the likelihood and its value do depend on η_1 , however, the set of points we need to build the convex hull does not depend on the value of η_1 . Considering $\eta_1 = \arg \max_{\eta_1} (\max_{\eta_2} \ell_{\hat{\tau}(\cdot), n}(\eta_1, \eta_2))$ we have $\hat{\tau}(\cdot) = \hat{\tau}(\eta_1)$ and we recover the desired result for $\hat{\tau}(\cdot)$.

Let us now consider the s first coordinates of x_t . We call x'_t the vector of \mathbb{R}^s containing the first s coordinates of x_t and define $P'(\tau) = (\tau, \sum_{t=1}^{\tau} x'_t)$. Now, using the previous result, the change maximizing the likelihood restricted to the first s coordinates is on the hull of $P'(\tau)$ and therefore also on the hull of $P(\tau)$. The same argument applies to any other choice of s coordinates, and thus will apply to the set that maximises the sparse log-likelihood.

B.4 Proof of Theorem 6

The proof comes from applying results of Kabluchko et al. [2017]. To do so we need to prove that the random walk $\{P(\tau)\}_{\tau \in \{1, \dots, n-1\}} = \{(\tau, \sum_{t=1}^{\tau} x_t)\}_{\tau \in \{1, \dots, n-1\}}$ satisfies two properties, (Ex) and (GP) defined below.

- (Ex) For any permutation σ of the set $\{1, \dots, n-1\}$, we have the distributional equality

$$\{(1, x_{\tau})\}_{\tau \in \{1, \dots, n-1\}} \stackrel{D}{=} \{(1, x_{\tau'})\}_{\tau' \in \sigma}$$

- (GP) Any $p+1$ vectors of the form $(\tau, \sum_{t=1}^{\tau} x_t)$ are almost surely linearly independent.

We show this in the following lemma.

Lemma 2. *Assuming that all x_τ^d are independent and identically distributed with a continuous distribution, the properties (Ex) and (GP) of Kabluchko et al. [2017] are satisfied.*

Proof. In the case where all x_τ^d are independent and identically distributed, the property (Ex) holds. To show that property (GP) holds, consider time $n \geq p + 2$ and choose any indices $\tau_1, \dots, \tau_{p+1}$ such that $0 < \tau_1 < \dots < \tau_{p+1} < n$. We define the following variables for $d = 1, \dots, p + 1$:

$$S_d = \left(\tau_d, \sum_{t=1}^{\tau_d} x_t \right) \in \mathbb{R}^{p+1}, \quad M_d = S_d - S_{d-1}, \quad \text{with } S_0 = 0.$$

It can be observed that $S_d = \sum_{k \leq d} M_k$ for any $d = 1, \dots, p + 1$. Therefore, the linear independence of S_1, \dots, S_{p+1} is equivalent to the linear independence of M_1, \dots, M_{p+1} . We denote the matrix of size $(p + 1) \times (p + 1)$ where its d -th column is M_d as M . Consider its transpose matrix M^T . Its first column-vector is filled with integers between 1 and $n - 1$. Linear algebra shows that proving linear independence for column vectors in M or in M^T is equivalent. The last p column vectors in M^T are drawn independently with a continuous density and thus are almost surely linearly independent, spanning a hyperplane of dimension p . The probability that a point in \mathbb{R}^{p+1} , the first column vector of M^T , is in this span is 0. In conclusion, for any given n , there are finitely many matrices M to consider, and their probabilities satisfy (GP), ensuring that property (GP) holds. \square

Based on Lemma 2 properties (Ex) and (GP) hold and we can apply formula (2) from Kabluchko et al. [2017] on the expected values of U_n^p and V_n^p . This completes the proof of Theorem 6.

Remark 2. *Theorem 6 gives the expectation for i.i.d. observations. One might wonder what happens if there is a changepoint in the distribution at $i < n$. Note that the points on the hull $\{P(\tau)\}_{\tau \in \{1, \dots, n-1\}}$ are necessarily on the hull of $\{P(\tau)\}_{\tau \in \{1, \dots, i\}}$ or on the hull of $\{P(\tau)\}_{\tau \in \{i+1, \dots, n-1\}}$. Thus applying the theorem on all points from 1 to i and from $i + 1$ to $n - 1$ we expect at most $\mathbb{E}(V_{i+1}^p) + \mathbb{E}(V_{n-i}^p) \leq 2\mathbb{E}(V_n^p)$ points on the hull (as the expectation of V_i^p is increasing with i). Thus if there is a changepoint (and assuming we have not stopped because the GLR statistics is lower than the specified threshold) the expected number of candidate changepoints is still in $\mathcal{O}(\log(n)^p)$.*

B.5 Empirical validation of the bound of Theorem 6

We empirically tested the validity of Theorem 6 for $p \leq 5$. We use the Gaussian distribution as an example of a distribution with continuous density and independent dimensions. To be specific, for p from 1 to 5, we simulated time series $x_{1:n}$, with $x_t \sim \mathcal{N}_p(0, I_p)$ i.i.d. We varied the time series length from $2^{10} + 1 (\approx 10^3)$ to $2^{23} + 1 (\approx 8 \times 10^6)$ and simulated 100 data sets for each length. We used the QuickHull algorithm Barber et al. [1996] implemented in the R package `geometry` Habel et al. [2023] to evaluate the number of faces and vertices of the convex hull of $\{P(\tau)\}_{\tau \in \{1, \dots, n-1\}}$. It can be seen in Figure 10 that the observed number of faces and vertices are close to their theoretical expectations (from Theorem 6). Additional details on the calculations of the Stirling numbers are provided in Supplementary Material E.

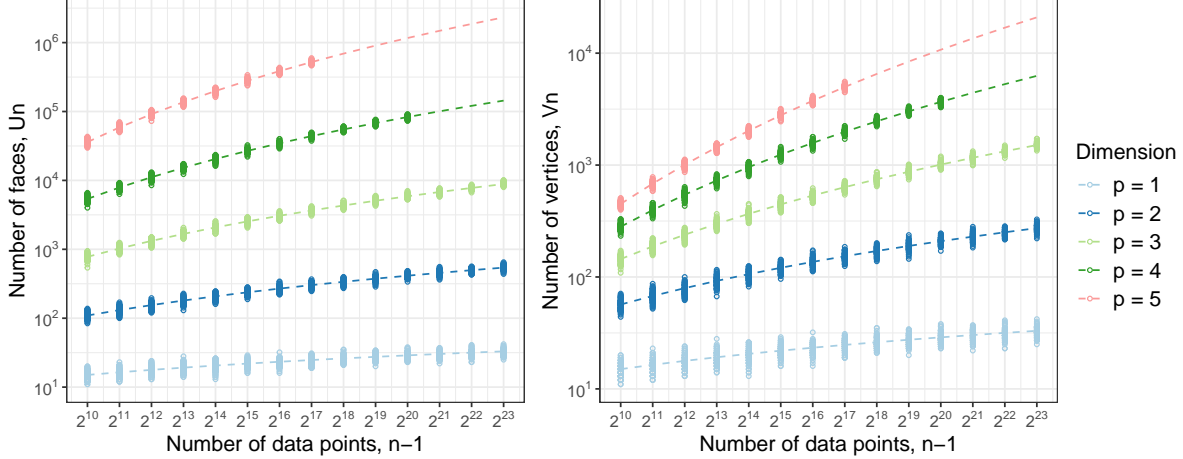


Figure 10: The number of faces (left) and vertices (right) of the convex hull of $\{P(\tau)\}_{\tau \in \{1, \dots, n-1\}}$ for dimension $1 \leq p \leq 5$. We simulated 100 i.i.d. Gaussian data $\mathcal{N}_p(0, I_p)$ for n from $(2^{10} + 1)$ to $(2^{23} + 1)$. Dashed lines correspond to the expected number of faces (left) and vertices (right) presented in Theorem 6. We consider a maximum running time of 40 minutes for the QuickHull algorithm. This is why some results for $p = 4$ and 5 for large number of observations are missing.

The proof of Theorem 6 depends on the fact that the distribution is continuous. We thus empirically tested the robustness of the expectations to this assumption by considering time series drawn with a discrete i.i.d. Poisson distribution. The results closely resemble the Gaussian case and details can be found in Section F.1.

C Exponential Family Models

Examples of models and change-types covered by our setting are given in Table 4. Our algorithms can also deal with data where different components of a multivariate stream are from different models.

Our setting also covers the change in mean (θ_1) and variance (θ_2) (so $p'' = 2$) of a Gaussian signal in \mathbb{R} (so $p' = 1$). In this slightly more complex case we have $p' \neq p = 2$ and we can define s, r, A' and B' as follows

$$\theta = (\theta_1, \theta_2), \quad \eta = \left(\frac{\theta_1}{\theta_2}, -\frac{1}{2\theta_2} \right), \quad s(y) = (y, y^2), \quad A'(\eta) = \frac{\theta_1^2}{\theta_2} - \log(\theta_2), \quad B'(x) = \log(2\pi).$$

D Index Set Equality

The equality $\mathcal{F}_{\mathcal{T}} = \mathcal{G}_{\mathcal{T}}$ can be proved with weaker conditions on A than those of Theorem 2. This equality has a simple geometric interpretation: to be true, any half-line in $Im(A) \times \mathcal{D}_A$ has to intersect the manifold defined by $\{(A(\mu), \mu), \mu \in \mathcal{D}_A\}$.

Theorem 7. *If A is continuous and defined on a cone with $Im(A) = \mathbb{R}^+$ such that $A(0) = 0$, $\nabla A(0) = 0$ and $\lim_{\|\mu\| \rightarrow \infty} \frac{A(\mu)}{\|\mu\|} = +\infty$ we have $\mathcal{F}_{\mathcal{T}} = \mathcal{G}_{\mathcal{T}}$.*

Table 4: Modelling a change in the mean of a p -variate data with independent Gaussian (known variance), Poisson, Binomial, Exponential, and Pareto type-I errors. Examples of distributions from the natural exponential family with a parameter θ in \mathbb{R}^p and the corresponding forms of the functions s , r , A' , and B' . Without loss of generality, the variance of the Gaussian model is assumed to be 1 for all dimensions. The number of trials is assumed to be m for all dimensions in the Binomial model. For the Pareto type-I model, the minimum value for each dimension, denoted y_m , is assumed to be known.

Distribution	$\eta := r(\theta)$	$x := s(y)$	$A'(\eta)$	$B'(x)$
Gaussian (changes in mean)	θ	y	$\ \eta\ ^2$	$\ x\ ^2 + \log(2\pi)^p$
Poisson	$\log \theta$	y	$2 \langle e^\eta, \mathbf{1}_p \rangle$	$2 \langle \log x!, \mathbf{1}_p \rangle$
Binomial	$\log \frac{\theta}{1-\theta}$	y	$2m \langle \log(1 + e^\eta), \mathbf{1}_p \rangle$	$-2 \left\langle \log \binom{m}{x}, \mathbf{1}_p \right\rangle$
Exponential	$-\theta$	y	$-2 \langle \log(-\eta), \mathbf{1}_p \rangle$	0
Pareto type-I	$-\theta - 1$	$\log(y)$	$-2 \langle \log(-1 - \eta), \mathbf{1}_p \rangle + 2 \langle 1 + \eta, \log(y_m) \rangle$	0

Proof. Consider τ in $\mathcal{G}_\mathcal{T}$. For all $\tau' \neq \tau$, the inverse image of the open set $(0, +\infty)$ by linear functions $g_\tau - g_{\tau'}$ is a non-empty intersection of half-spaces. Moreover, there exists $(\lambda_0, \mu_0) \in \text{Im}(A) \times \mathcal{D}_A$ such that for all $\tau' \neq \tau$ in \mathcal{T} we have: $g_\tau(\lambda_0, \mu_0) > g_{\tau'}(\lambda_0, \mu_0)$. For $\alpha > 0$ we get by linearity

$$g_\tau(\alpha\lambda_0, \alpha\mu_0) = \alpha g_\tau(\lambda_0, \mu_0) > \alpha g_{\tau'}(\lambda_0, \mu_0) = g_{\tau'}(\alpha\lambda_0, \alpha\mu_0).$$

Therefore, as all points of the half-line $\{\alpha(\lambda_0, \mu_0), \alpha > 0\}$ belong to this set, it shows that index τ is optimal on an open polyhedral cone.

Suppose that for the considered (λ_0, μ_0) , there exists $\alpha_0 > 0$ such that $\lambda_0 = \frac{A(\alpha_0\mu_0)}{\alpha_0}$ then $\alpha_0\mu_0$ is a value in the cone \mathcal{D}_A verifying all the constraints $f_\tau(\alpha_0\mu_0) > f_{\tau'}(\alpha_0\mu_0)$, so that τ also belongs to $\mathcal{F}_\mathcal{T}$. In geometric terms, this means that any half-line in the polyhedral cone associated with index τ intersects the manifold defined by $\{(A(\mu), \mu), \mu \in \mathcal{D}_A\}$.

It remains to prove that the proposed assumptions over A are sufficient to find such an alpha proving the set equality. We consider the same half-line $\{\alpha(\lambda_0, \mu_0), \alpha > 0\}$. By a linear approximation about 0, we have $A(\epsilon) = A(0) + \langle \epsilon, \nabla A(0) \rangle + o(\|\epsilon\|) = o(\|\epsilon\|)$ and locally, we get $A(\alpha\mu_0) = o(\|\alpha\mu_0\|) < \alpha\lambda_0$ for small α . Notice that as $\text{Im}(A) = \mathbb{R}^+$ and the cone is open, we have $\lambda_0 > 0$ and can choose $\|\mu_0\| > 0$. The half-line is therefore above the manifold (" $(\alpha\lambda_0, \alpha\mu_0) > (A(\alpha\mu_0), \alpha\mu_0)$ ").

Using condition $\lim_{\alpha \rightarrow \infty} \frac{A(\alpha\mu_0)}{\|\alpha\mu_0\|} = +\infty$, continuity of A and previous local result $\frac{A(\alpha\mu_0)}{\|\alpha\mu_0\|} = o(1)$ for small α , it shows that there exists α_0 such that $\frac{A(\alpha_0\mu_0)}{\|\alpha_0\mu_0\|} = \frac{\lambda_0}{\|\mu_0\|}$ (as $\frac{\lambda_0}{\|\mu_0\|} > 0$). Thus $(\alpha_0\lambda_0, \alpha_0\mu_0) = (A(\alpha_0\mu_0), \alpha_0\mu_0)$ which leads to $f_\tau(\alpha_0\mu_0) > f_{\tau'}(\alpha_0\mu_0)$ and index τ is in $\mathcal{F}_\mathcal{T}$. \square

E Stirling numbers of the first kind in terms of the harmonic series

To obtain numerical values of U_n^p and V_n^p of the convex hull of $\{P(\tau)\}_{\tau \in \{1, \dots, n-1\}}$ for $1 \leq p \leq 5$ we need to know the expressions of $\begin{bmatrix} n \\ m \end{bmatrix}$ for $m = 0, \dots, 6$. As shown in Adamchik [1997],

the general formula for the Stirling numbers of the first kind in terms of the harmonic series is

$$\begin{bmatrix} n \\ m \end{bmatrix} = \frac{(n-1)!}{(m-1)!} \omega(n, m-1). \quad (14)$$

The ω -sequence is defined recursively by

$$\omega(n, m) = \mathbb{1}_{m=0} + \sum_{k=0}^{m-1} (1-m)_k \sigma_{k+1} \omega(n, m-1-k),$$

where $\sigma_{k+1} = \sum_{i=1}^{n-1} \frac{1}{i^{k+1}}$ is the partial sums of the harmonic series $\{\frac{1}{i^{k+1}}\}_{i=1,2,\dots}$ and $(1-m)_k$ are the Pochhammer symbols. Applying (14) for $m = 0, \dots, 6$, we get

$$\begin{aligned} \begin{bmatrix} n \\ 0 \end{bmatrix} &= 1, & \begin{bmatrix} n \\ 1 \end{bmatrix} &= (n-1)!, & \begin{bmatrix} n \\ 2 \end{bmatrix} &= (n-1)! \sigma_1, \\ \begin{bmatrix} n \\ 3 \end{bmatrix} &= \frac{(n-1)!}{2} (\sigma_1^2 - \sigma_2), & \begin{bmatrix} n \\ 4 \end{bmatrix} &= (n-1)! \left(\frac{\sigma_1^3}{6} - \frac{\sigma_1 \sigma_2}{2} + \frac{\sigma_3}{3} \right), \\ \begin{bmatrix} n \\ 5 \end{bmatrix} &= (n-1)! \left(\frac{\sigma_1^4}{24} - \frac{\sigma_1^2 \sigma_2}{4} + \frac{\sigma_1 \sigma_3}{3} + \frac{\sigma_2^2}{8} - \frac{\sigma_4}{4} \right), \\ \begin{bmatrix} n \\ 6 \end{bmatrix} &= (n-1)! \left(\frac{\sigma_1^5}{120} - \frac{\sigma_1^3 \sigma_2}{12} + \frac{\sigma_1^2 \sigma_3}{6} + \frac{\sigma_1 \sigma_2^2}{8} - \frac{\sigma_1 \sigma_4}{4} - \frac{\sigma_2 \sigma_3}{6} + \frac{\sigma_5}{5} \right). \end{aligned}$$

F Additional Empirical evaluations

F.1 Multidimensional Poisson Model

We simulated time series with each data-point simulated a p independent Poisson random variables with mean 1. We varied p and n as in Section B.5. Using the same procedure as in Section B.5, we evaluate the number of faces and vertices of the convex hull $\{P(\tau)\}_{\tau \in \{1, \dots, n-1\}}$. The results are presented in Figure 11. We note that the results are similar to the Gaussian case (see Figure 10).

Next, using the same procedure as in Section 4.3, we evaluated the run times of MdFOCuS for a known or unknown pre-change parameter for Poisson distribution. The results are presented in Figure 12. We note that the results are similar to the Gaussian case (see Figure 3).

F.2 Run time as a function of a slope parameter

We consider the empirical run times of the MdFOCuS algorithm with a known pre-change parameter η_1 as a function of parameter α . Using the implementation of Algorithm 1 for a change in the mean of multi-dimensional Gaussian signal (see Table 4) in R/C++ using the `qhull` library we studied how the α parameter affects its run time. To do this, we generate 100 time series with $n = 10^5$ data points, with each data point an independent realisation of a standard p -dimensional Gaussian random variable, in dimension $p = 1, 2$ and

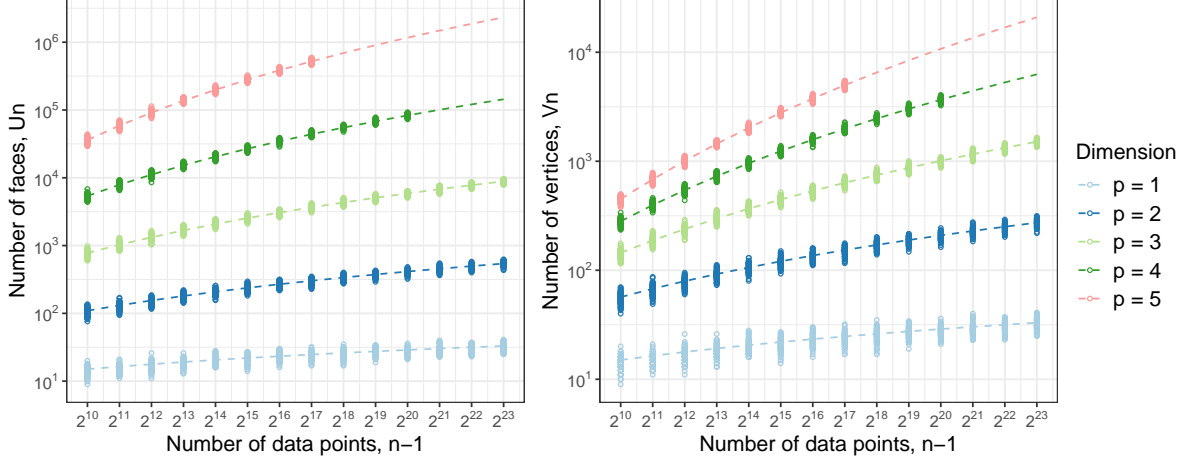


Figure 11: The number of faces (left) and vertices (right) of the convex hull built from the set of points $\{P(i)\}_{i \in \{1, \dots, n-1\}}$ for dimension $1 \leq p \leq 5$. Results averaged over 100 realisations of independent p -dimensional Poisson random variables with mean 1 data. Dashed lines correspond to the expected number of faces (left) and vertices (right) presented in Theorem 6. We consider a maximum running time of 40 minutes for the `Quickhull` algorithm, hence no data points for $p = 4$ and 5 for large numbers of observations.

3. In Figure 13 we report the average run time as a function of α for MdFOCuS for the pre-change parameter known case. The value of `maxSize` was always initialised to $p + 2$ and β was always set to 1. We observe a minimum run time for α in $[2, 4]$. As a consequence, in the rest of the simulations we always set α to 2.

F.3 50-dimensional time series, controlled by false positive rate

We present, in Table 5, an additional simulation study to compare the simple one-dimensional multivariate implementation proposed by Romano et al. [2023] (here called FOCuS), with the high-dimensional approximation for MdFOCuS using the two-dimensional approximation of the convex hull alongside the partial likelihood ratio statistic (see Section 4.5 and subsection H). To facilitate a fair comparison, we tune the thresholds of all methods to achieve the same pre-change false positive rate of 0.01. We applied a Bonferroni correction to cope with multiple thresholds. The simulation scenarios mirror those of the main study but with the changepoint occurring at time 10000. This is to emphasize the impact of the approximations. We expect the two-dimensional approximation to outperform the one-dimensional approximation proposed by Romano et al. [2023], particularly for small-magnitude changes. However, as observed in the main study, the original FOCuS method is still superior when observing a change in one dimension, as, despite in that case the statistics being equal, its threshold is slightly lower (because it considers fewer statistics in total).

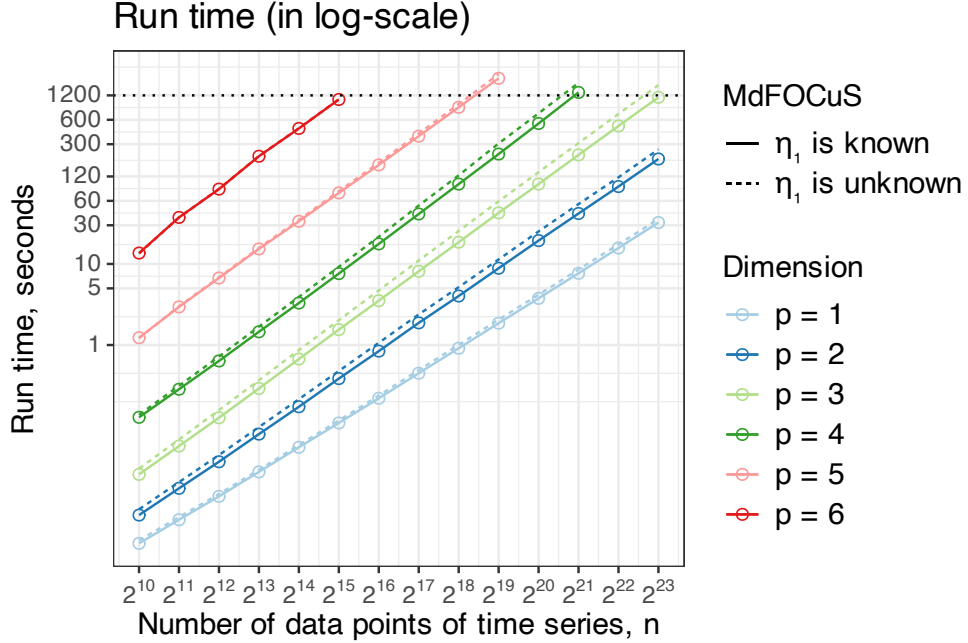


Figure 12: Run times in seconds of MdFOCuS with known (dashed line) and unknown (full line) pre-change parameter η_1 , both with $\alpha = 2$, $\beta = 1$ and $maxSize = 14$, in dimension $p = 1, \dots, 6$ using time series $x_{1:n}$ simulated from the independent Poisson model. Run times are averaged over 100 data sets. We considered a maximum running time of 20 minutes (horizontal dotted black line) for the algorithms, hence no run times for $p = 4, 5$ and 6 for large numbers of observations. The slope of the curves was obtained using a simple linear regression: for known η_1 : ≈ 1.013 ($p = 1$), ≈ 1.126 ($p = 2$), ≈ 1.192 ($p = 3$), ≈ 1.210 ($p = 4$), ≈ 1.172 ($p = 5$) and ≈ 1.250 ($p = 6$); for unknown η_1 : ≈ 1.018 ($p = 1$), ≈ 1.138 ($p = 2$), ≈ 1.213 ($p = 3$), ≈ 1.240 ($p = 4$), ≈ 1.190 ($p = 5$) and ≈ 1.254 ($p = 6$).

F.4 Additional Plug-in estimated methods

The following Tables 6, 7 and 8 show detection delays for various amount of training data prior to the monitoring period, and can be used to aid the comparison of the methods in the main simulation study.

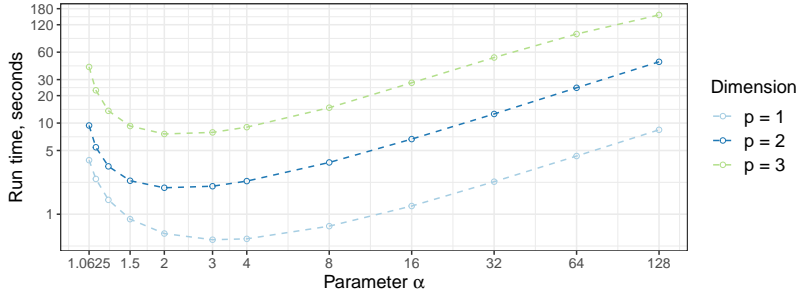


Figure 13: Run time of MdFOCuS as a function of α for p -variate time series with $n = 10^5$ data points in dimension $p = 1, 2$ and 3 . Results averaged over 100 simulations.

G Dyadic MdFOCuS : an algorithm with a quasi-linear expected complexity

In this appendix we present an algorithm for online changepoint detection. In essence, as in the MdFOCuS algorithm of the main text, it maintains a set of points that is slightly larger than the set of points on the hull. It does so applying the `QuickHull` (or any convex hull) algorithm on successive and non-overlapping deterministic chunks of the points. This deterministic choice of chunks is likely sub-optimal but it allows for a precise quantification of the expected complexity of the algorithm under the assumption of Theorem 6 and under the assumption that the convex hull algorithm is at worst quadratic. To be specific we obtain a $\mathcal{O}(n \log(n)^{p+1})$ bound on the expected time complexity.

We begin with two preliminary results. The first is a crude bound on the expectation of the square of the number of points on the convex hull of n points (that is $(V_n^p)^2$ following the notation of Section 4.2) under the assumptions of Theorem 6. The second result bounds the expected complexity of computing the hull of $2n$ points if we already know the points on the hull of the first n points and the last n points. In all that follows we will assume that Assumptions 1 and 2 described in the main text are true. For ease of reading, we repeat them here.

Assumption 1. *In any dimension $p \geq 1$, there are positive constants c_1 and c_2 for which the expected number of vertices, $\mathbb{E}[V_n^p]$, can be bounded as follows:*

$$\mathbb{E}[V_n^p] \leq c_1 \log(n)^p + c_2.$$

This is true under the conditions of Theorem 6 and Corollary 1.

Remember we define $Time(n)$ to be the worst-case time complexity of finding the convex hull of n points.

Assumption 2. *For our convex hull algorithm we are using there exist two positive constants c_3 and c_4 such that $Time(n) \leq c_3 n^2 + c_4$.*

The assumption on the quadratic complexity is true for `QuickHull` for $p \leq 2$ [Barber et al., 1996] and using the algorithm of Chazelle [1993] it is true for $p \leq 3$. We now state our bound on the expectation of the square of the number of points on the hull V_n^p .

Table 5: Average detection delay with 50-dimensional time series for a change at time $t = 10000$. Pre-change parameter is known on the left, and unknown on the right. Best results per row are highlighted in bold. Results are by controlling the false positive rate. FOCuS (est 500) estimates the pre-change parameter from training data of length 500.

magnitude	sparsity	Pre-change Known		Pre-change Unknown		
		FOCuS	MdFOCuS	FOCuS (est 500)	FOCuS	MdFOCuS
0.125	1	2347.52	2426.00	9980.48	3161.26	3295.96
0.125	5	3524.53	3380.42	9981.21	6088.01	5375.96
0.125	10	3997.59	3814.82	9980.60	7299.97	6362.57
0.125	25	4288.27	4224.50	9979.48	8474.92	7479.11
0.125	50	4509.18	4362.75	9982.43	8874.72	7853.60
0.250	1	584.56	599.49	8932.53	627.85	644.16
0.250	5	977.95	871.53	9779.57	1167.59	970.06
0.250	10	1159.92	996.14	9845.31	1504.27	1117.59
0.250	25	1299.23	1096.57	9893.83	1925.51	1322.48
0.250	50	1350.10	1163.00	9893.97	2216.25	1400.04
0.500	1	147.73	151.25	2711.61	150.70	153.69
0.500	5	245.45	212.26	4818.17	259.12	215.56
0.500	10	310.56	247.15	6139.80	357.20	257.50
0.500	25	358.34	274.32	7015.92	458.89	290.81
0.500	50	385.03	290.86	7316.34	534.77	309.12
0.750	1	66.55	67.78	1194.15	66.86	68.33
0.750	5	109.84	96.61	2208.06	112.88	97.46
0.750	10	146.07	111.96	3022.77	159.63	113.25
0.750	25	173.78	123.47	3713.07	208.40	128.58
0.750	50	185.83	129.10	3977.72	239.54	134.76
1.000	1	37.90	39.03	668.06	38.16	39.06
1.000	5	63.03	55.14	1254.92	64.23	55.10
1.000	10	84.73	63.52	1759.00	89.73	63.96
1.000	25	102.40	73.13	2226.95	120.41	75.12
1.000	50	109.77	75.73	2427.92	139.52	78.38
2.000	1	10.22	10.52	166.65	10.20	10.52
2.000	5	17.22	14.74	314.93	17.38	14.75
2.000	10	23.24	17.06	456.38	24.11	17.10
2.000	25	28.69	18.96	596.50	32.33	19.40
2.000	50	31.41	19.90	662.81	38.29	20.43

Lemma 3.

$$\mathbb{E}[(V_n^p)^2] \leq c_1 n \log(n)^p + c_2 n. \quad (15)$$

Table 6: Average detection delay with 3-dimensional time series for a change at time $t = 1000$. Comparison of pre-change mean known methods with plug-in oracle value (ora) against plug-in mean estimate for differing training data sizes (500, 250 and 100).

magnitude	sparsity	FOCuS (ora)	FOCuS (est 500)	FOCuS (est 250)	FOCuS (est 100)	ocd (ora)	ocd (est 500)	ocd (est 250)	ocd (est 100)
0.125	1	786.67	1162.32	1470.76	2253.81	1227.57	1721.56	1783.41	2490.39
0.125	2	791.36	1327.92	1693.06	2302.31	1421.54	2043.79	1987.04	2415.50
0.125	3	859.03	1352.66	1723.76	2329.12	1496.18	2046.77	2097.23	2337.57
0.250	1	250.58	325.38	470.69	1251.62	227.18	330.05	430.33	1102.87
0.250	2	253.56	364.98	556.86	1375.63	268.86	389.39	516.28	1173.38
0.250	3	273.92	401.56	630.94	1433.94	300.69	468.61	559.66	1204.47
0.500	1	65.85	80.59	113.75	312.64	56.46	71.71	83.90	177.84
0.500	2	71.85	92.22	132.99	354.26	65.18	81.19	96.50	181.77
0.500	3	79.21	106.81	155.61	396.17	74.50	92.76	103.97	169.63
0.750	1	31.80	37.30	50.73	133.10	28.95	34.93	39.46	67.11
0.750	2	34.66	42.69	61.46	154.01	32.52	38.90	43.47	70.93
0.750	3	37.19	49.00	71.75	172.62	35.43	42.38	46.40	68.02
1.000	1	18.51	21.83	29.18	73.23	18.87	21.98	24.16	35.99
1.000	2	20.30	25.32	34.55	86.22	20.45	23.68	25.45	37.82
1.000	3	21.68	27.79	40.03	98.67	21.52	24.70	26.23	37.56
2.000	1	5.35	6.18	8.06	19.03	6.40	7.06	7.12	9.14
2.000	2	5.97	7.18	9.46	22.10	6.64	7.10	7.25	9.64
2.000	3	6.51	7.89	10.62	24.63	6.80	7.32	7.41	9.48

Table 7: Average detection delay with 5-dimensional time series for a change at time $t = 1000$. Comparison of pre-change mean known methods with plug-in oracle value (ora) against plug-in mean estimate for differing training data sizes (500, 250 and 100).

magnitude	sparsity	FOCuS (ora)	FOCuS (est 500)	FOCuS (est 250)	FOCuS (est 100)	ocd (ora)	ocd (est 500)	ocd (est 250)	ocd (est 100)
0.125	1	833.11	1488.18	2219.97	2706.40	911.17	1583.01	2458.66	3081.32
0.125	2	892.82	1534.50	2221.24	2685.51	1106.68	1599.44	2441.70	3074.78
0.125	3	925.08	1615.20	2255.65	2691.14	1101.38	1706.65	2493.92	3053.87
0.125	4	835.44	1472.64	2102.15	2629.56	1059.06	1472.04	2296.26	3005.94
0.125	5	953.85	1584.83	2228.96	2701.14	1297.37	1621.73	2448.01	3046.09
0.250	1	259.75	435.84	871.35	1775.82	229.64	387.14	1064.11	2268.01
0.250	2	281.77	493.33	963.88	1839.07	253.79	424.68	1084.21	2281.61
0.250	3	297.41	517.02	1004.43	1924.93	287.10	446.80	1077.31	2336.42
0.250	4	260.23	471.25	918.63	1819.93	265.40	365.10	852.33	2140.46
0.250	5	304.13	541.09	1023.24	1988.96	309.16	439.40	1000.05	2350.21
0.500	1	72.98	107.78	206.83	537.16	64.74	96.04	247.08	763.99
0.500	2	84.75	128.09	243.50	610.94	73.93	108.04	253.56	828.08
0.500	3	91.31	139.43	267.82	655.26	83.54	110.27	252.69	846.27
0.500	4	80.89	131.85	250.83	608.11	75.94	93.22	199.82	686.05
0.500	5	95.41	154.27	293.72	703.96	89.48	111.43	235.87	841.18
0.750	1	33.44	47.69	91.82	228.48	32.98	44.57	108.72	341.20
0.750	2	39.21	58.27	113.10	267.93	36.22	48.39	113.74	380.14
0.750	3	41.29	64.95	124.88	294.45	38.61	49.04	110.91	381.23
0.750	4	37.03	61.29	116.62	277.83	34.71	41.39	87.09	305.25
0.750	5	45.65	74.44	137.55	326.77	42.24	50.95	104.84	366.27
1.000	1	19.63	27.77	51.75	128.48	21.37	27.25	62.33	209.80
1.000	2	22.88	33.47	63.86	151.84	22.88	28.27	62.99	220.30
1.000	3	24.67	36.48	71.35	167.23	23.65	28.63	62.24	216.61
1.000	4	22.45	35.42	67.41	156.69	20.32	23.52	49.88	167.50
1.000	5	27.18	43.05	81.02	186.18	25.07	29.31	61.01	204.52
2.000	1	5.79	7.72	13.40	31.86	7.25	7.97	15.78	56.68
2.000	2	6.88	9.16	16.57	38.91	7.47	8.06	15.66	55.90
2.000	3	7.21	10.14	18.62	42.92	7.33	8.15	15.74	53.75
2.000	4	6.64	10.04	17.92	40.14	6.10	6.66	12.99	42.46
2.000	5	7.91	11.92	21.30	48.72	7.40	8.10	15.55	52.15

Proof. V_n^p is bounded by 0 and $n - 1$. It follows that

$$\mathbb{E}[(V_n^p)^2] = \sum_{i=0}^n \mathbb{P}(V_n^p = i) i^2 \leq n \sum_{i=0}^n \mathbb{P}(V_n^p = i) i \leq n \mathbb{E}[V_n^p] \leq c_1 n \log(n)^p + c_2 n. \quad (16)$$

Table 8: Average detection delay with 100-dimensional time series for a change at time $t = 1000$. Comparison of pre-change mean known methods with plug-in oracle value (ora) against plug-in mean estimate for differing training data sizes (500, 250 and 100).

magnitude	sparsity	FOCuS (ora)	FOCuS (est 500)	FOCuS (est 250)	FOCuS (est 100)	ocd (ora)	ocd (est 500)	ocd (est 250)	ocd (est 100)
0.125	1	1417.15	3269.06	3459.08	3615.97	1171.63	3361.86	3546.43	3696.77
0.125	5	1881.10	3429.84	3497.94	3604.75	1627.00	3490.18	3595.24	3691.58
0.125	10	2084.84	3450.20	3501.48	3607.64	1940.41	3510.97	3595.46	3695.33
0.125	50	2252.48	3473.50	3494.67	3611.70	2386.98	3547.64	3591.96	3704.31
0.125	100	2323.59	3505.76	3507.66	3610.74	2431.51	3564.11	3599.24	3705.24
0.250	1	389.11	1552.28	2659.50	3436.24	335.95	1643.28	2841.37	3542.47
0.250	5	641.18	2363.35	3054.36	3510.27	505.39	2477.35	3232.02	3607.01
0.250	10	789.27	2590.60	3178.29	3518.29	595.10	2706.71	3334.21	3622.86
0.250	50	1057.30	3026.93	3323.17	3549.36	827.30	3142.73	3453.27	3662.49
0.250	100	1080.26	3101.34	3346.50	3544.06	891.09	3200.56	3476.58	3650.38
0.500	1	105.79	359.11	721.53	1798.04	104.79	411.98	859.71	2132.81
0.500	5	169.93	661.68	1297.63	2580.08	139.23	708.99	1449.56	2809.88
0.500	10	232.04	900.72	1653.97	2868.20	170.03	958.71	1850.22	3077.24
0.500	50	357.90	1730.82	2480.88	3231.38	239.08	1868.74	2719.69	3408.29
0.500	100	372.34	1916.38	2611.86	3237.55	244.07	2093.59	2841.33	3407.16
0.750	1	47.78	158.37	310.89	761.25	57.56	228.43	461.51	1138.50
0.750	5	75.34	297.90	580.05	1389.39	73.47	354.74	715.73	1704.61
0.750	10	104.45	408.77	798.60	1831.94	84.16	458.03	925.56	2114.73
0.750	50	184.09	958.18	1626.21	2651.16	114.29	1036.67	1836.28	2889.70
0.750	100	193.77	1156.00	1823.30	2730.10	115.21	1283.48	2074.96	2956.24
1.000	1	27.12	89.54	173.04	419.58	38.67	158.25	317.49	772.93
1.000	5	43.72	168.56	325.28	791.73	46.07	237.96	476.20	1142.06
1.000	10	60.36	235.29	458.62	1094.25	50.77	298.13	599.74	1422.86
1.000	50	109.11	580.49	1074.41	2036.18	66.02	630.09	1218.93	2284.94
1.000	100	116.60	747.72	1288.45	2190.83	67.59	823.90	1466.28	2453.87
2.000	1	7.58	22.69	43.03	103.23	12.93	71.01	142.00	341.47
2.000	5	12.92	42.04	82.41	199.48	13.80	101.81	203.48	485.40
2.000	10	16.46	60.00	117.67	283.82	14.80	124.40	250.44	594.86
2.000	50	31.85	162.50	315.56	734.61	18.08	226.70	451.59	1021.58
2.000	100	34.28	222.17	422.46	920.47	18.34	255.33	493.39	1104.39

We get the last inequality with Assumption 1. \square

We now state our bound on the complexity of merging the hull of two successive chunks.

Lemma 4. *Consider we have $2n$ data points. Assume we know \mathcal{W}_1 the index of the points on the hull of $\{P(\tau)\}_{1 \leq \tau \leq n}$ and \mathcal{W}_2 the index of the points on the hull of $\{P(\tau)\}_{n+1 \leq \tau \leq 2n}$. Under the condition of Corollary 1 and Assumption 2 computing the index of the points on the hull of $\{P(\tau)\}_{1 \leq \tau \leq 2n}$ can be done in less than $4c_1c_3n(\log n)^p + 4c_2c_3n + c_4$ time.*

Proof. We will compute those points as the points on the hull of $\{P(\tau)\}_{\tau \in \mathcal{W}_1 \cup \mathcal{W}_2}$. By Assumption 2 the time complexity of processing these $|\mathcal{W}_1| + |\mathcal{W}_2|$ points is

$$\text{Time}(|\mathcal{W}_1| + |\mathcal{W}_2|) \leq c_3(|\mathcal{W}_1| + |\mathcal{W}_2|)^2 + c_4 \leq 2c_3(|\mathcal{W}_1|^2 + |\mathcal{W}_2|^2) + c_4.$$

Now taking the expectation with respect to the number of points in \mathcal{W}_1 and \mathcal{W}_2 , and noting that under the assumption of Corollary 1 the distribution of $|\mathcal{W}_1|$ is the same as the distribution of $|\mathcal{W}_2|$ we get

$$\mathbb{E}(\text{Time}(|\mathcal{W}_1| + |\mathcal{W}_2|)) \leq 4c_3\mathbb{E}(|\mathcal{W}_1|^2) + c_4.$$

Using (15) we get that the expected complexity is

$$\mathbb{E}(\text{Time}(|\mathcal{W}_1| + |\mathcal{W}_2|)) \leq 4c_1c_3n(\log n)^p + 4c_2c_3n + c_4. \quad (17)$$

\square

Now, before presenting the dyadic algorithm, we explain the set of candidates it considers and how this set is updated.

G.1 Dyadic algorithm: Set of candidates

Recall that at time n we would ideally only store the vertices on the hull of $\{P(\tau)\}_{\tau < n}$. In the following algorithm we store the vertices on the hull of chunks of the form $\{k2^q + 1, \dots, (k+1)2^q\}$ for all $q \geq q_{min}$. To be specific, we consider the base 2 description of n : $n = \sum_{q=0}^{\lfloor \log_2(n) \rfloor} \bar{n}_q 2^q$, with $\bar{n}_q = 0$ or 1, and define for q in $\{0, \dots, \lfloor \log_2(n-1) \rfloor\}$ the subset \mathcal{U}_n^q of $\{1, \dots, n-1\}$ as

$$\mathcal{U}_n^q = \left\{ \tau \mid \sum_{q'=q+1}^{\lfloor \log_2(n-1) \rfloor} \overline{(n-1)}_{q'} 2^{q'} < \tau \leq \sum_{q'=q}^{\lfloor \log_2(n-1) \rfloor} \overline{(n-1)}_{q'} 2^{q'} \right\},$$

with the convention that for $q = \lfloor \log_2(n-1) \rfloor$ the sum $\sum_{q'=q+1}^{\lfloor \log_2(n-1) \rfloor} \overline{(n-1)}_{q'} 2^{q'}$ is equal to 0.

We provide a few examples of these sets for $n = 20$ to $n = 31$ in Table 9. It can be observed that often \mathcal{U}_n^q differs from \mathcal{U}_{n+1}^q only for small values of q .

Table 9: A few \mathcal{U}_n^q sets.

n	$q = 4$	$q = 3$	$q = 2$	$q = 1$	$q = 0$
31	$\{1, \dots, 16\}$	$\{17, \dots, 24\}$	$\{25, \dots, 28\}$	$\{29, 30\}$	\emptyset
30	$\{1, \dots, 16\}$	$\{17, \dots, 24\}$	$\{25, \dots, 28\}$	\emptyset	$\{29\}$
29	$\{1, \dots, 16\}$	$\{17, \dots, 24\}$	$\{25, \dots, 28\}$	\emptyset	\emptyset
28	$\{1, \dots, 16\}$	$\{17, \dots, 24\}$	\emptyset	$\{25, 26\}$	$\{27\}$
27	$\{1, \dots, 16\}$	$\{17, \dots, 24\}$	\emptyset	$\{25, 26\}$	\emptyset
26	$\{1, \dots, 16\}$	$\{17, \dots, 24\}$	\emptyset	\emptyset	$\{25\}$
25	$\{1, \dots, 16\}$	$\{17, \dots, 24\}$	\emptyset	\emptyset	\emptyset
24	$\{1, \dots, 16\}$	\emptyset	$\{17, \dots, 20\}$	$\{21, 22\}$	$\{23\}$
23	$\{1, \dots, 16\}$	\emptyset	$\{17, \dots, 20\}$	$\{21, 22\}$	\emptyset
22	$\{1, \dots, 16\}$	\emptyset	$\{17, \dots, 20\}$	\emptyset	$\{21\}$
21	$\{1, \dots, 16\}$	\emptyset	$\{17, \dots, 20\}$	\emptyset	\emptyset
20	$\{1, \dots, 16\}$	\emptyset	\emptyset	$\{17, 18\}$	$\{19\}$

For any $q_{min} \leq \lfloor \log_2(n-1) \rfloor$

$$\bigcup_{q=q_{min}}^{\lfloor \log_2(n-1) \rfloor} \mathcal{U}_n^q \cup \left\{ \tau \mid \sum_{q'=q_{min}}^{\lfloor \log_2(n-1) \rfloor} \overline{(n-1)}_{q'} 2^{q'} < \tau \leq n-1 \right\},$$

is a partition of $\{1, \dots, n-1\}$. The right-side set of this partition has at most $2^{q_{min}}$ elements. We use this partition to update the set of candidates. To be specific our algorithm maintains

$$\mathcal{T}_n = \bigcup_{q=q_{min}}^{\lfloor \log_2(n-1) \rfloor} \mathcal{W}_n^q \cup \left(\left\{ P(\tau) \mid \sum_{q'=q_{min}}^{\lfloor \log_2(n-1) \rfloor} \overline{(n-1)}_{q'} 2^{q'} < \tau \leq n-1 \right\} \right),$$

with $\mathcal{W}_n^q = \text{HULL}(\{P(\tau)\}_{\tau \in \mathcal{U}_n^q})$. Note that \mathcal{T}_n contains all the points (or index of the points) on the hull of $\{P(\tau)\}_{\tau \in \{1, \dots, n-1\}}$.

In the next paragraphs, we bound the expected number of points in \mathcal{T}_n and then explain how we compute \mathcal{T}_{n+1} from \mathcal{T}_n .

Lemma 5. *For a fixed q_{min} , under Assumption 1 we have*

$$\mathbb{E}(|\mathcal{T}_n|) \leq 2c_1(\log n)^{p+1} + 2c_2 \log n + 2^{q_{min}}. \quad (18)$$

Proof. For a fixed q_{min} using Assumption 1 for all \mathcal{U}_n^q we get that

$$\begin{aligned} \mathbb{E}(|\mathcal{T}_n|) &\leq \sum_{q=q_{min}}^{\lfloor \log_2(n-1) \rfloor} (c_1(\log 2^q)^p + c_2) + 2^{q_{min}} \\ &\leq \sum_{q=q_{min}}^{\lfloor \log_2(n-1) \rfloor} (c_1(\log n)^p + c_2) + 2^{q_{min}} \\ &\leq 2c_1(\log n)^{p+1} + 2c_2 \log n + 2^{q_{min}}. \end{aligned}$$

We get the last inequality using the fact that we sum over at most $\log_2(n)$ terms and $1/\log(2) \leq 2$. \square

G.2 Dyadic algorithm: Updating the set of candidates

To compute \mathcal{T}_{n+1} from scratch we need to apply the hull algorithm on all \mathcal{U}_{n+1}^q for $q \geq q_{min}$. Assuming we have already computed \mathcal{T}_n computing \mathcal{T}_{n+1} is a bit easier. This is because it is often the case that $\mathcal{U}_{n+1}^q = \mathcal{U}_n^q$. Therefore we directly get the indices of the point on the hull of \mathcal{U}_{n+1}^q as $\mathcal{U}_n^q \cap \mathcal{T}_n$ because

$$\mathcal{W}_n^q = \text{HULL}(\{P(\tau)\}_{\tau \in \mathcal{U}_n^q}) = \mathcal{U}_n^q \cap \mathcal{T}_n.$$

Algorithm 2 formalise this idea and iteratively merge chunks of size 2^q to take advantage of Lemma 4.

Algorithm 2 Update of the set of candidates

- 1: **Input :** n and $\mathcal{T} = \mathcal{T}_n$
 - 2: $\mathcal{T} \leftarrow \mathcal{T} \cup \{n\}$
 - 3: $q \leftarrow q_{min}$
 - 4: **while** $\text{remainder}(n/2^q) = 0$ **do**
 - 5: $\mathcal{T}' \leftarrow \{\tau \in \mathcal{T} \mid \tau > n - 2^q\}$
 - 6: $\mathcal{T}'' \leftarrow \text{QUICKHULL}(\{P(\tau)\}_{\tau \in \mathcal{T}'})$
 - 7: $\mathcal{T} \leftarrow \mathcal{T} \setminus (\mathcal{T}' \setminus \mathcal{T}'')$ \triangleright discard vertices in \mathcal{T}' not in \mathcal{T}''
 - 8: $q \leftarrow q + 1$
 - 9: **end while**
 - 10: **return** $\mathcal{T} = \mathcal{T}_{n+1}$
-

Remark 3. In Algorithm 2 we assume that if the set of points $\{P(\tau)\}_{\tau \in \mathcal{T}'}$ doesn't define a proper volume in dimension $p+1$ then the output of $\text{QUICKHULL}(\{P(\tau)\}_{\tau \in \mathcal{T}'})$ is simply \mathcal{T}' . If we choose q_{\min} such that $2^{q_{\min}}$ is larger than $p+2$ this is unlikely to happen for data drawn from a distribution with a continuous density.

We now continue with an informal description of Algorithm 2. Looking at line 4 when we include a new data point $n+1$ two cases can happen.

- n is not a multiple of $2^{q_{\min}}$. In that case for all $q \geq q_{\min}$ we have $\mathcal{U}_{n+1}^q = \mathcal{U}_n^q$. We just need to add n as a possible changepoint to \mathcal{T}_n to recover \mathcal{T}_{n+1} . This was done in line 2.
- n is a multiple of $2^{q_{\min}}$. In that case for some $q \geq q_{\min}$ we have that \mathcal{U}_{n+1}^q is different from \mathcal{U}_n^q . We therefore need to update the set of points using the hull algorithm.

For the later case let us define $q_n \geq q_{\min}$ as the largest integer such that 2^{q_n} divides n . Before we explain the update of lines 5, 6, and 7 note the following facts.

- In base 2, n ends with a one followed by q_n zeros. In other words $\overline{n}_{q_n} = 1$ and for all $q < q_n$ $\overline{n}_q = 0$. Thus all \mathcal{U}_{n+1}^q with $q < q_n$ should be empty and $\mathcal{U}_{n+1}^{q_n}$ is not.
- In base 2, $n-1$ ends with a zero followed by q_n ones. In other words $\overline{(n-1)}_{q_n} = 0$ and for all $q < q_n$ $\overline{(n-1)}_q = 1$. Thus all \mathcal{U}_n^q with $q < q_n$ are not empty.
- We know the index of the points on the hull for all sets of indices \mathcal{U}_n^q with $q < q_n$:

$$\mathcal{W}_n^q = \text{HULL}(\{P(\tau)\}_{\tau \in \mathcal{U}_n^q}) = \mathcal{U}_n^q \cap \mathcal{T}_n.$$

- Finally, $\mathcal{U}_{n+1}^{q_n} = (\cup_{q_{\min} \leq q < q_n} \mathcal{U}_n^q) \cup \{\tau | n - 2^{q_{\min}} < \tau \leq n\}$.

Our goal is to get the point (or indices of these points) on the hull of $P(\tau)$ for τ in $\mathcal{U}_{n+1}^{q_n}$. To exploit the merging bound of (17) Algorithm 2 iteratively applies the hull algorithm on larger and larger chunks of the data trimming the points that are not on the hull. In the while loop, from lines 4 to 9, of Algorithm 2 we can distinguish two cases.

1. For $q = q_{\min}$ on lines 5 and 6 the algorithm applies the hull algorithm on the 2^q right-most points: $\text{HULL}(\{P(\tau)\}_{n-2^q < \tau \leq n})$. It then discards on line 7 all indices larger than $n - 2^q$ that are not on this hull.
2. If $q_{\min} < q \leq q_n$ on lines 5 and 6 the algorithm applies the hull algorithm on indices that are larger than $n - 2^q$. In essence it is applying the hull algorithm on the points computed during the previous while step (indices larger than $n - 2^{q-1}$ and in \mathcal{T}) with those of $\mathcal{W}_n^q = \text{HULL}(\{P(\tau)\}_{\tau \in \mathcal{U}_n^q}) = \mathcal{U}_n^q \cap \mathcal{T}_n$ (indices between $n - 2^q$ and $n - 2^{q-1}$, and in \mathcal{T}). A bit more formally, calling \mathcal{W}_{n+1}^q the output of line 6 (\mathcal{T}'') at step q of the while loop, we are merging \mathcal{W}_n^q and \mathcal{W}_{n+1}^{q-1} as follows:

$$\mathcal{W}_{n+1}^q = \text{HULL}\left(\{P(\tau)\}_{\tau \in \mathcal{W}_n^q \cup \mathcal{W}_{n+1}^{q-1}}\right).$$

On line 7 the algorithm is discarding all indices larger than $n - 2^q$ that are not on this hull \mathcal{W}_{n+1}^q .

Proceeding in such a way at each step we merge the points on the hull of two successive chunks of size 2^{q-1} to recover the points on the hull of a chunk of size 2^q . Figure 14 is a schematic representation of these successive fusions (applications of the hull algorithm).

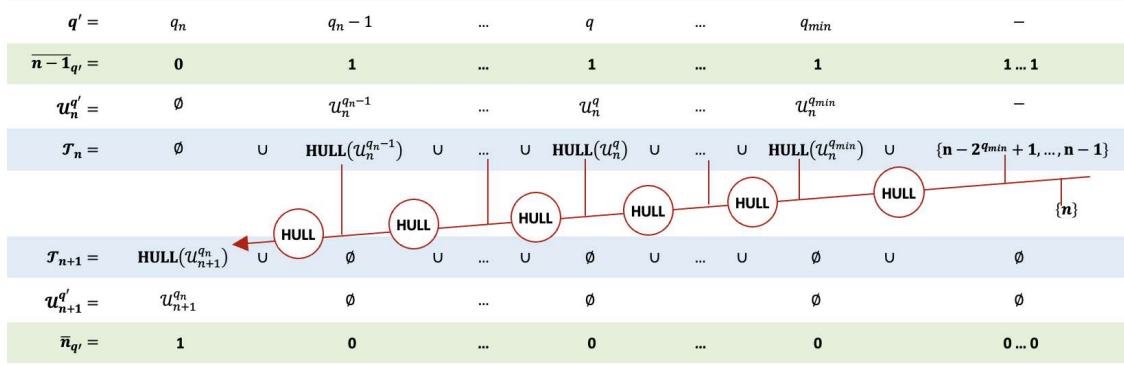


Figure 14: Schematic representation of the while loop of Algorithm 2 for q_n being the largest q such that 2^q divides n . First applying the hull algorithm on $\{n - 2^{q_{min}} + 1, \dots, n\}$ (on the right) following the red arrow we iteratively aggregate the result with the hull of points in \mathcal{U}_n^q to recover the point on the hull of $\mathcal{U}_{n+1}^{q_n}$ (on the left). In such a way we effectively retrieve \mathcal{T}_{n+1} as all \mathcal{U}_{n+1}^q are empty for $q < q_n$.

Example 1. *In this paragraph we explain how the algorithm proceeds for $n = 24$ and $q_{min} = 2$. In base 2, $n - 1 = 10111$. Therefore (see the definition of set \mathcal{T}_n) we already computed the points on the hull of $P(\tau)$ for τ in $\mathcal{U}_{24}^4 = \{1, \dots, 16\}$ and τ in $\mathcal{U}_{24}^2 = \{17, \dots, 20\}$, and additionally we store all indices τ larger than $24 - 2^2 : \{21, 22, 23\}$. When we include a new observation $n + 1 = 25$, we need to include a possible change at $n = 24$, and here is what we do with the while loop (starting with $q = 2$):*

- for $q = 2$: we run *Quickhull* on points with indices strictly larger than 20 : $\{21, 22, 23, 24\}$;
- for $q = 3$: to recover \mathcal{U}_{25}^3 we run *Quickhull* on points with indices strictly larger than 16 that is the points obtained in the previous step ($q = 2$) union those of the hull of \mathcal{U}_{24}^2 (that were computed for $n + 1 = 21$ as the point on the hull of \mathcal{U}_{21}^2).
- for $q = 4$: we stop as the remainder of $24/2^4$ is not 0.

We are now ready to give the proof of Lemma 1 in the main text, which we rewrite here to ease reading.

Lemma 1. *Under Assumptions 1 and 2, the expected time complexity of Algorithm 2 is $\mathcal{O}(n \log(n)^{p+1})$.*

Proof. Considering all time steps up to $n + 1$ the algorithm used the *QuickHull* algorithm on all successive (and nonoverlapping) chunks of size 2^q for q larger than q_{min} and smaller than $\lfloor \log_2(n) \rfloor$.

For the smallest scale, $n' = 2^{q_{min}}$, we have $n/2^{q_{min}}$ chunks and run *QuickHull* on all points. Using Assumption 2, the worst time per chunk is less than $c_3(2^{q_{min}})^2 + c_4$, and

summing overall chunks we get $nc_32^{q_{min}} + \frac{nc_4}{2^{q_{min}}}$ operations. So at the smallest, scale the computational cost is $\mathcal{O}(n)$.

We will now successively consider all larger scales $n' = 2^q$ for $q_{min} < q \leq \lfloor \log_2(n) \rfloor$. The hull of a chunk of size $n' = 2^q$ is obtained by combining the hulls of two smaller chunks of size 2^{q-1} . For any such chunk, we can thus exploit Lemma 4 and (17) with $|\mathcal{W}_1| = |\mathcal{W}_2| = n'/2 = 2^{q-1}$ and we get

$$\mathbb{E}(\text{Time}(|\mathcal{W}_1| + |\mathcal{W}_2|)) \leq 4c_1c_32^{q-1}(\log 2^{q-1})^p + 4c_2c_32^{q-1} + c_4.$$

Multiplying by $n/2^q$ to consider all chunks of size 2^q , we get that the time to process scale 2^q is

$$\begin{aligned} \frac{n}{2^q} (4c_1c_32^{q-1}(\log 2^{q-1})^p + 4c_2c_32^{q-1} + c_4) &\leq 4c_1c_3\frac{n}{2}(\log 2^{q-1})^p + 4c_2c_3\frac{n}{2} + c_4\frac{n}{2^q} \\ &\leq 4c_1c_3\frac{n}{2}(\log n)^p + 4c_2c_3\frac{n}{2} + c_4\frac{n}{2^q}. \end{aligned}$$

So the computational cost at scale 2^q is $\mathcal{O}(n \log(n)^p)$. Multiplying by $\log_2(n)$ to consider all scales, we get the desired result. \square

G.3 MdFOCuS with dyadic update

The MdFOCuS Algorithm implementing this update of the set of candidates is presented in Algorithm 3. Combining Lemma 5 and 1 we get an overall complexity that is $\mathcal{O}(n \log(n)^{p+1})$.

Algorithm 3 MdFOCuS Dyadic algorithm

- 1: **Input 1:** $\{x_t\}_{t=1,2,\dots}$ p -variate independent time series; *thrs* threshold; η_1 pre-change parameter (if known); q_{min} min power 2 scale at which we run `QuickHull`
 - 2: **Outputs:** stopping time n and maximum likelihood change: $\hat{\tau}(\cdot)$ or $\hat{\tau}(\eta_1)$
 - 3: $GLR \leftarrow -\infty$, $\mathcal{T} \leftarrow \emptyset$, $n \leftarrow 1$
 - 4: **while** ($GLR < \textit{thrs}$) **do**
 - 5: $n \leftarrow n + 1$
 - 6: $\mathcal{T} \leftarrow \mathcal{T} \cup \{n - 1\}$
 - 7: $\hat{m} \leftarrow \max_{\tau \in \mathcal{T}} \{\max_{\eta_1, \eta_2} \ell_{\tau, n}(\eta_1, \eta_2)\}$ $\triangleright \eta_1$ is fixed if pre-change known
 - 8: $GLR \leftarrow \hat{m} - \max_{\eta_1, \eta_2} \ell_{n, n}(\eta_1, \eta_2)$ $\triangleright \eta_1$ is fixed if pre-change known
 - 9: $q \leftarrow q_{min}$
 - 10: **while** $\text{REMAINDER}(\frac{n-1}{2^q}) = 0$ **do**
 - 11: $\mathcal{T}' \leftarrow \{\tau \in \mathcal{T} | \tau > n - 2^q\}$
 - 12: $\mathcal{T}'' \leftarrow \text{QUICKHULL}(\{P(\tau)\}_{\tau \in \mathcal{T}'})$
 - 13: $\mathcal{T} \leftarrow \mathcal{T} \setminus (\mathcal{T}' \setminus \mathcal{T}'')$ \triangleright discard vertices in \mathcal{T}' not in \mathcal{T}''
 - 14: $q \leftarrow q + 1$
 - 15: **end while**
 - 16: **end while**
 - 17: **return** n and GLR
-

We implemented Algorithm 3 for a change in the mean of multi-dimensional Gaussian signal in R/C++ using the `qhull` library. We evaluate the empirical run times of Algorithm

3 with various values of q_{min} using the profiles of Supplementary Material F.2. In Figure 15 we report the average run time as a function of the dyadic parameter q_{min} for MdFOCuS for a known value of η_1 with the dyadic update and values of q_{min} in $3, \dots, 12$. We observe a minimum run time for $q_{min} = 6$ for $p = 1$, $q_{min} = 7$ for $p = 2$ and $q_{min} = 8$ for $p = 3$. As a consequence in the rest of the simulations we always set q_{min} to $p + 5$.

Using the simulation framework of Section 4.3 we evaluated the run times of MdFOCuS with dyadic update for dimension $p = 1$ to $p = 3$ and compared it with run times of MdFOCuS. The average run times are presented in Figure 16. Dyadic MdFOCuS is slower than MdFOCuS, by about a factor of 2.

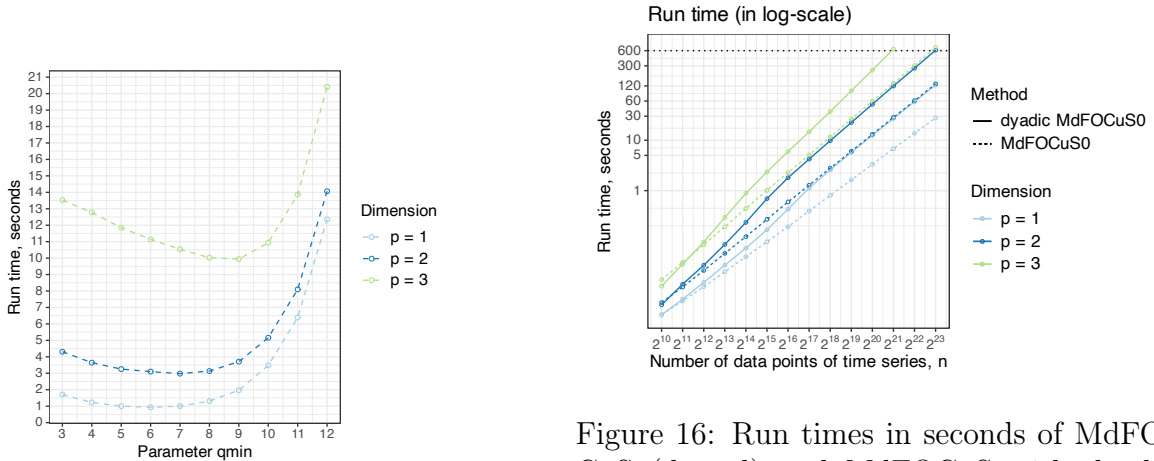


Figure 15: Run time of MdFOCuS with dyadic update as a function of q_{min} for p -variate time series with $n = 10^5$ data points in dimension $p = 1, 2$ and 3 . We simulated 100 i.i.d. Gaussian data $\mathcal{N}_p(0, I_p)$ and report the average run time.

Figure 16: Run times in seconds of MdFOCuS (dotted) and MdFOCuS with dyadic update (full) both with $q_{min} = 5 + p$ in dimension $p = 1, 2$ and 3 using time series $x_{1:n}$ (without change, $x_t \sim \mathcal{N}_p(0, I_p)$ i.i.d.). Run times are averaged over 100 data sets. We considered a maximum running time of 10 minutes for the algorithms. That is why we do not report run times for $p = 3$ for large signals.

H An approximation for large p

Based on Theorem 6 and its corollary at step n we expect Algorithm 1 to store $\mathcal{O}(\log^p(n))$ candidates. Considering the calculation of the full and sparse maximum likelihood in lines 7 and 8 should thus have a complexity of $\mathcal{O}(p \log^p(n))$. The power $\log(n)^p$ is problematic making the algorithm impractical for p larger than 6, as exemplified in Figure 3.

Here we propose a heuristic solution to this problem. Our idea is to get a subset of the point on the hull considering projections on at most \tilde{p} variates.

For any ordered subset $S = \{S_1, \dots, S_{|S|}\}$ of $\{1, \dots, p\}$, with $|S|$ the size of S , we define $x_t^{[S]}$ the vector in $\mathbb{R}^{|S|}$ such that the i -th coordinate of $x_t^{[S]}$ is the S_i -coordinate of x_t . We

then define $P^{[S]}(\tau)$ accordingly:

$$P^{[S]}(\tau) = \left(\tau, \sum_{t=1}^{\tau} x_t^{[S]} \right).$$

Similarly, we call $\mathcal{T}_n^{[S]}$ the set of index τ such that $P^{[S]}(\tau)$ is on the hull of $\{P^{[S]}(\tau)\}_{\tau \in \{1, \dots, n-1\}}$. We now consider \mathcal{S} a subset of all subsets of $\{1, \dots, p\}$ (i.e $\mathcal{P}(\{1, \dots, p\})$ or $2^{\{1, \dots, p\}}$) and we get an inner approximation of \mathcal{T}_n taking a union over all $\mathcal{T}_n^{[S]}$:

$$\cup_{S \in \mathcal{S}} \mathcal{T}_n^{[S]} \subseteq \mathcal{T}_n.$$

In our simulations as a minimalist implementation of this approximation we considered $\tilde{p} = 2$ and subsets of the form $\{\tilde{p}j+1, \dots, \tilde{p}j+\tilde{p}\}$ for $j \leq p/\tilde{p}$. We have p/\tilde{p} such sets and under the condition of Theorem 6 we thus expect to store $\mathcal{O}(p \log^{\tilde{p}}(n))$ candidate changepoints rather than $\mathcal{O}(\log^p(n))$ with the exact Algorithm 1. For $p = 100$ and $n = 10000$, our approximation with $\tilde{p} = 2$, implemented in R runs on average in less than 100 seconds. More generally it can be seen in Figure 4 that run times of our R implementation of MdFOCuS, and our 2d approximation for larger p are comparable to ocd Chen et al. [2022].

Algorithm 4 MdFOCuS \tilde{p} d approximation

- 1: **Input 1:** p -variate independent time series $\{x_t\}_{t=1,2,\dots}$
 - 2: **Input 2:** threshold $thrs$ and η_1 if known pre-change parameter
 - 3: **Input 3:** \mathcal{S} a subset of all subsets of $\{1, \dots, p\}$, with for all $S \in \mathcal{S} : |S| \leq \tilde{p}$
 - 4: **Input 4:** For all $S \in \mathcal{S}$ a list of index $\mathcal{T}^{[S]}$
 - 5: **Input 5:** For all $S \in \mathcal{S}$ a S specific pruning index $maxSize^{[S]}$
 - 6: **Output:** stopping time n and approximated maximum likelihood change : $\hat{\tau}(\cdot)$ or $\hat{\tau}(\eta_1)$
 - 7: $GLR \leftarrow -\infty$, For all $S \in \mathcal{S} \quad \mathcal{T}^{[S]} \leftarrow \emptyset, \quad n \leftarrow 0$
 - 8: **while** ($GLR < thrs$) **do**
 - 9: $n \leftarrow n + 1$
 - 10: **for all** $S \in \mathcal{S}$ **do**
 - 11: $\mathcal{T}^{[S]} \leftarrow \mathcal{T}^{[S]} \cup \{n - 1\}$
 - 12: **end for**
 - 13: $\hat{m} \leftarrow \max_{\tau \in \cup_{S \in \mathcal{S}} \mathcal{T}^{[S]}} \{\max_{\eta_1, \eta_2} \ell_{\tau, n}(\eta_1, \eta_2)\}$ $\triangleright \eta_1$ is fixed if pre-change known
 - 14: $GLR \leftarrow \hat{m} - \max_{\eta_1, \eta_2} \ell_{n, n}(\eta_1, \eta_2)$ $\triangleright \eta_1$ is fixed if pre-change known
 - 15: **for all** $S \in \mathcal{S}$ **do**
 - 16: **if** ($|\mathcal{T}^{[S]}| > maxSize^{[S]}$) **then**
 - 17: $\mathcal{T}^{[S]} \leftarrow \text{QUICKHULL}(\{P^{[S]}(\tau)\}_{\tau \in \mathcal{T}^{[S]}})$
 - 18: $maxSize^{[S]} \leftarrow \lfloor \alpha |\mathcal{T}^{[S]}| + \beta \rfloor$
 - 19: **end if**
 - 20: **end for**
 - 21: **end while**
 - 22: **return** n and GLR
-

I On the probability of false alarms, average-run-length and average detection delay in the multivariate Gaussian case

I.1 Definitions and problem statement

In this section, we consider the multivariate Gaussian case. That is, we consider a sequence $\{y_t\}_{t=1,2,\dots}$ with elements in \mathbb{R}^p , with $y_t = \mu_t + \varepsilon_t$, and ε_t i.i.d $\mathcal{N}_p(0, I_p)$. At time n , for any possible change $\tau < n$, we consider two types of statistics:

- Ranked-based statistics, $S_{\tau,n}^{\#s}$, considering the s dimensions with the most evidence for a change at τ ;
- Threshold-based statistics, $S_{\tau,n}^{(a)}$, considering, as in Chen et al. [2022], only the dimensions for which the evidence for a change exceeds the threshold a .

To formally present these statistics, we first define the unsorted per-dimension evidence for a change at τ at time n knowing the pre-change mean to be 0, $O_{\tau,n}^i(0)$ or not knowing the pre-change mean, $O_{\tau,n}^i(\cdot)$:

$$O_{\tau,n}^i(0) = \frac{1}{\sqrt{n-\tau}} \sum_{t=\tau+1}^n \varepsilon_t^i, \quad O_{\tau,n}^i(\cdot) = \sqrt{\frac{\tau(n-\tau)}{n}} \left(\frac{1}{n-\tau} \sum_{t=\tau+1}^n \varepsilon_t^i - \frac{1}{\tau} \sum_{t=1}^{\tau} \varepsilon_t^i \right),$$

where ε_t^i is the i -th coordinate of ε_t in \mathbb{R}^p . We also define the sorted per-dimension evidence for a change at τ at time n , $O_{\tau,n}^{\#j}(0)$ as the j -th highest value out of all $O_{\tau,n}^i(0)$. Similarly, for the unknown pre-change mean scenario, we define $O_{\tau,n}^{\#j}(\cdot)$ as the j -th highest value out of all $O_{\tau,n}^i(\cdot)$. Based on that, we now define our rank and threshold-based statistics knowing the pre-change mean to be 0 as:

$$S_{\tau,n}^{\#s}(0) = \sum_{j=1}^s (O_{\tau,n}^{\#j}(0))^2 \quad \text{and} \quad S_{\tau,n}^{(a)}(0) = \sum_{i=1}^p (O_{\tau,n}^i(0))^2 \mathbb{1}_{|O_{\tau,n}^i(0)| \geq a}, \quad (19)$$

where $\mathbb{1}$ denotes the indicator function. We define similar statistics if the pre-change mean is not known:

$$S_{\tau,n}^{\#s}(\cdot) = \sum_{j=1}^s (O_{\tau,n}^{\#j}(\cdot))^2 \quad \text{and} \quad S_{\tau,n}^{(a)}(\cdot) = \sum_{i=1}^p (O_{\tau,n}^i(\cdot))^2 \mathbb{1}_{|O_{\tau,n}^i(\cdot)| \geq a}. \quad (20)$$

For simplicity, when this does not cause confusion, we will omit the (0) and (.) notations. It will sometimes make sense to consider separately the ranked-1 statistics $S_{\tau,n}^{\#1}$. We will refer to $S_{m,n}^{\#p} = S_{m,n}^{(a=0)}$ as the dense statistic.

First we summarise our results:

1. For all ranked and thresholded statistics, we provide, in Section I.2, time-varying thresholds to control their false alarm rate. To be specific, considering a generic ranked or thresholded statistic $\tilde{S}_{\tau,n}$, we provide a varying threshold $c_n(\alpha)$ for which:

$$\mathbb{P}(\exists \tau < n \in \mathbb{N} \text{ such that } \tilde{S}_{\tau,n} \geq c_n(\alpha)) \leq \alpha.$$

Importantly, our thresholds are also valid if the pre-change mean is unknown. As a byproduct, we can calibrate a fixed threshold to control the Average Run Length, γ . That is, we can define a threshold $c(\gamma)$ such that if all μ_t are equal to 0 then $E(\tilde{T}) \geq \gamma$, where \tilde{T} is the first time our generic statistic passes the threshold.

2. Second, in Section I.3, assuming the pre-change mean is known, and for a fixed threshold c , we control using the optional stopping time theorem, the Average Detection Delay (ADD). To be specific, assuming $\mu_t = 0$ for all $t \leq \tau^*$ and $\mu_t = \delta$ otherwise we get a bound on

$$\sup_{y_1, \dots, y_{\tau^*}} \mathbb{E}(\tilde{T} - \tau^* | \tilde{T} \geq \tau^*),$$

involving only $\|\delta\|$ and the threshold. For thresholded statistics, the same result holds by replacing c by $c + pa^2$ (see remark 6).

3. Finally, in Section I.4, for all our ranked and thresholded statistics, assuming we know the pre-change mean, we provide probabilistic bounds on the Detection Delay. To be specific, again assuming $\mu_t = 0$ for all $t \leq \tau^*$ and $\mu_t = \delta$ otherwise, we bound with probability $1 - \alpha$ the detection time, $\tilde{T} - \tau^*$, by a term involving only $\|\delta\|$, the threshold, and α .

I.2 Probability of false alarms for all statistics

Proposition 8. *For a sequence without change : $y_t = \varepsilon_t$ with ε_t i.i.d. $\mathcal{N}_p(0, I_p)$. Considering a time-varying $x_n(\alpha) = 4 \log(n) - \log(\alpha)$, we can control the false alarm rate of ranked and thresholded statistics at level α . That is for a generic statistic $\tilde{S}_{\tau,n}$ we control:*

$$\mathbb{P}(\exists \tau < n \in \mathbb{N} \text{ such that } \tilde{S}_{\tau,n} \geq c_n(\alpha)) \leq \alpha,$$

using the thresholds in table 10.

Statistic $\tilde{S}_{\tau,n}$	Threshold $c_n(\alpha)$
$S_{\tau,n}^{\#1}$	$2x_n(\alpha) + 2 \log(2p)$
$S_{\tau,n}^{\#s}$	$2(x_n(\alpha) + \log\binom{p}{s}) + 2\sqrt{s(x_n(\alpha) + \log\binom{p}{s})} + s$
$S_{\tau,n}^{(a)}$	$4x_n(\alpha) + 6pe^{-a^2/8}$

Table 10: Probability bounds for our statistics with $x_n(\alpha) = 4 \log(n) - \log(\alpha)$

Proof. We follow Step 1 and Step 2 of the proof of Theorem 1 in Yu et al. [2023] using the peeling concentration bounds of our Lemma 7. \square

Importantly, when using MdFOCuS, one typically considers several statistics. Denoting $\#Stats$ the number of statistics, we control simultaneously all of them at level α' taking $\alpha = \alpha'/\#Stats$ in the thresholds of Table 10.

Remark 4. Using Proposition 8 we can also control the Average Run Length (ARL) using a fixed threshold, c . Consider the Rank-1 statistic, $S_{\tau,n}^{\#1}$, as an example. We note that its threshold $2x_n(\alpha) + 2\log(2p)$ increases with n . Thus, using a fixed threshold $c = 2x_N(\alpha) + 2\log(p)$ for all time n , the probability of stopping before N is less than α , and therefore the ARL is larger than $(1 - \alpha)N$. To control the ARL at any desired level γ , it suffices to choose a sufficiently large N and a sufficiently small probability α such that $(1 - \alpha)N \geq \gamma$.

I.3 Average detection delay for a fixed threshold and knowing the pre-change mean

In this section, we assume that a change in mean occurs immediately after time τ^* . Assume that we are using the dense statistic $S_{\tau,n}^{\#p}(0) = S_{\tau,n}^{(0)}(0)$ with a fixed threshold (following Remark 4) and let T be the first time that our test statistic exceeds the threshold. The average detection delay is defined as

$$ADD = \sup_{y_1, \dots, y_{\tau^*}} \mathbb{E}(T - \tau^* | T \geq \tau^*).$$

That is, it is the worst-case expected time from the change until it is detected, conditional on no detection before τ^* .

Lemma 6. For a change of size δ , with $\|\delta\|^2$ its Euclidean squared norm, the average detection delay for the dense statistic with a known pre-change mean ($S_{\tau,n}^{\#p}(0) = S_{\tau,n}^{(0)}(0)$) and a fixed threshold c satisfies

$$ADD \leq \frac{c + \|\delta\| \sqrt{8/\pi}}{\|\delta\|^2} + 1.$$

Proof. Let τ^* be the time of the change, and T the time at which the dense statistic first exceeds c . Consider the test statistic for a change at τ of size δ , which at time $\tau^* + t$, for $t = 1, 2, \dots$ is of the form:

$$A_t = \sum_{i=1}^t (2\delta^T y_{\tau^*+i} - \|\delta\|^2). \quad (21)$$

Note that $\max_{\delta} A_t = S_{\tau^*, \tau^*+t}^{\#p}$. Define $A_0 = 0$.

Now for any data $y_{1:t+\tau^*}$ we have $A_t \leq \max_{\tau=0}^{\tau^*+t-1} S_{\tau, t+\tau^*}^{\#p}(0)$. Let T' be the time that A_t first exceeds c . It follows that conditional on $T > \tau^*$, we have $T' \geq T - \tau^*$. Thus we can bound the ADD by $\mathbb{E}(T')$.

Denote each term in the sum on the right-hand side of (21) by a_i . We have these terms are independent, normally distributed with mean $\mathbb{E}(a_i) = \delta^T \delta = \|\delta\|^2$ and variance $4\|\delta\|^2$.

For each t it is trivial to see that $\mathbb{E}(|A_t|) < \infty$, and thus $A_t - t\|\delta\|^2$ is a Martingale. It is also straightforward to show that T' is a stopping time and $\mathbb{E}(T') < \infty$ so we can apply the optional stopping theorem. This gives

$$\mathbb{E}(A_{T'} - T'\|\delta\|^2) = 0.$$

Thus $\mathbb{E}(T') = \mathbb{E}(A_{T'})/\|\delta\|^2$. We can bound $\mathbb{E}(A_{T'})$ from above by considering the distribution of $A_{T'}$ conditional on $A_{T'-1}$. We have

$$\mathbb{E}(A_{T'} | A_{T'-1} = A) = \mathbb{E}\left(A + \|\delta\|^2 + \sqrt{4\|\delta\|^2}\epsilon \mid A + \|\delta\|^2 + \sqrt{4\|\delta\|^2}\epsilon \geq c\right),$$

where ϵ has a standard normal distribution. This expectation is monotone increasing in A , and as $A < c$ we can bound $\mathbb{E}(A_{T'})$ by the value of the conditional expectation in the limit as $A \rightarrow c$ from below. This gives

$$\mathbb{E}(A_{T'}) \leq \mathbb{E}(c + \|\delta\|^2 + \sqrt{2\|\delta\|^2}|\epsilon|) = c + \|\delta\|^2 + \sqrt{2\|\delta\|^2}\sqrt{\frac{2}{\pi}}.$$

The result follows. □

Remark 5. *It is simple to extend this result to get a bound on the ADD of any ranked statistics $S_{\tau,n}^{\#s}(0)$, because the same argument applies to any statistic that considers a given subset of s variates changing. Following the notation introduced in Appendix G (on the approximation), denoting R the subset of s variates that are changing, we would recover the same formula considering $y^{[R]}$ in \mathbb{R}^s and replacing $\|\delta\|$ by $\|\delta^{[R]}\|$.*

Remark 6. *The proof also applies to any thresholded statistics with threshold a . We replace c by $c + pa^2$ in the proof, note that $S_{\tau,n}^{\#p} - pa^2$ is always smaller than $S_{\tau,n}^{(a)}$ and the bound follows.*

I.4 Probabilistic bound on the Detection Delay for a fixed threshold and knowing the pre-change mean

In this section, we again assume that a change in mean occurs immediately after time τ^* , calling T the first time our statistic passes the threshold c_n we give probabilistic bounds on the detection delay $T - \tau^*$. We start with ranked statistics and then proceed with thresholded statistics.

Proposition 9. *Consider a change of size δ at time τ^* , that is $y_t = \varepsilon_t$ for $t \leq \tau^*$ and $y_t = \delta + \varepsilon_t$ for $t > \tau^*$ with $\varepsilon_t \sim \mathcal{N}(0, I_p)$ and $\|\delta\| > 0$. We denote T the first time the dense statistic, $S_{\tau,n}^{\#p}(0)$, passes the fixed positive threshold c . With probability at least $(1 - \alpha)$ the detection delay, $T - \tau^*$, is less than*

$$\frac{2c - 8 \log(\alpha/2)}{\|\delta\|^2}$$

In addition, if $c > p$, then with probability at least $(1 - \alpha)$,

$$T - \tau^* < \frac{2(c - p) + 2\sqrt{p \log(3/\alpha)} - 8 \log(\alpha/3)}{\|\delta\|^2}$$

Proof. We consider the statistic $S_{\tau^*, n}^{\#p}(0)$ for increasing n and apply Lemma 8 and find that for any time larger than the provided bound, the statistic would pass the threshold with probability at least $(1 - \alpha)$. Hence, the detection delay would be smaller with probability $(1 - \alpha)$. \square

Remark 7. It is simple to extend this result to get a bound on the detection delay of any ranked statistic $S_{\tau, n}^{\#s}(0)$. This is because the same argument applies to the statistic that considers any subset of s variates changing. Following the notation introduced in Appendix G (on the approximation), denoting R the subset of s variates that are changing, we would consider y^R in \mathbb{R}^s and recover the same formula replacing $\|\delta\|$ by $\|\delta^{[R]}\|$.

Using Lemma 8 we could get similar bounds for a time-varying threshold assuming it is positive, increasing, and concave thresholds.

Before providing bounds on the detection delay of thresholded statistics, we recall the notion of effective sparsity defined in Chen et al. [2022]. For any δ in \mathbb{R}^p such that $\|\delta\| > 0$ the effective sparsity $z(\delta)$ is the smallest integer in $\{2^0, 2^1, \dots, 2^{\lceil \log_2(p) \rceil}\}$ such that the set

$$\mathcal{Z}(\delta) = \{j \text{ such that } |\delta^j| > \|\delta\| / (z(\delta) \log_2(p))\},$$

has cardinality at least $z(\delta)$.

Proposition 10. Consider a change of size δ at time τ^* , that is $y_t = \varepsilon_t$ for $t \leq \tau^*$ and $y_t = \delta + \varepsilon_t$ for $t > \tau^*$ with $\varepsilon_t \sim \mathcal{N}(0, I_p)$ and $\|\delta\| > 0$. We denote T the first time the thresholded statistic, $S_{\tau, n}^{(a)}(0)$, passes the fixed threshold c . With probability at least $(1 - \alpha)$ the detection delay, $T - \tau^*$, is less than

$$\log_2(p) \max \left\{ \frac{2c - 8 \log(\alpha) + 8 \log(2(z(\delta) + 1))}{\|\delta\|^2}, \frac{2a^2 - 8 \log(\alpha) + 8 \log(2(z(\delta) + 1))}{\|\delta\|^2 / z(\delta)} \right\}$$

Proof. We consider a subset \mathcal{Z}' of size $z(\delta)$ of $\mathcal{Z}(\delta)$. All variates j in this subset validate the effective sparsity constraint: $|\delta_j| > \|\delta\| / (z(\delta) \log_2(p))$. We first lower bound the contribution to $S_{\tau, n}^{(a)}$ of all variates not in \mathcal{Z}' by 0. Then we consider a time large enough to ensure that simultaneously

- the contribution of each variates in \mathcal{Z}' passes the threshold a
- the sum of these $z(\delta)$ contributions passes the fixed threshold c .

To this end we use Lemma 8 exactly $z(\delta) + 1$ times:

- for each variates in \mathcal{Z}' the lemma applies replacing $\|\delta\|^2$ by $\frac{\|\delta\|^2}{z(\delta) \log_2(p)}$ and α by $\frac{\alpha}{z(\delta)+1}$ (in preparation for a union bound).

- for the sum the lemma applies replacing $\|\delta\|^2$ by $\frac{\|\delta\|^2}{\log_2(p)}$ and α by $\frac{\alpha}{z(\delta)+1}$. This is because, by definition of $z(\delta)$ the squared euclidean norm restricted to the variates in \mathcal{Z}' is such that $\|\delta^{[\mathcal{Z}']}\|^2 \geq \frac{\|\delta\|^2}{\log_2(p)}$.

We get the desired result on the detection delay by taking a union bound over these $z(\delta) + 1$ events. \square

Using Lemma 8 we could get similar bounds for a time-varying threshold assuming it is positive, increasing, and concave thresholds.

I.5 Some concentration bounds

In this subsection, we provide concentration bounds on our ranked and threshold-based statistics, respectively $S_{\tau,n}^{\#s}$ and $S_{\tau,n}^{(a)}$ defined in (19) and (20). These bounds are useful to control the run-length and the detection delay

First, exploiting the peeling argument of Yu et al. [2023] we provide bounds considering all possible values of τ and n which are useful to control the probability of false alarms (see Proposition 8). These bounds and their proof are valid for both the known and unknown pre-change mean scenarios. This is because if there is no change $O_{\tau,n}^i(0)$ and $O_{\tau,n}^i(\cdot)$ are both Gaussian with mean zero and variance one.

Lemma 7. *Assume ε_t are i.i.d. Gaussian with identity variance matrix. For α in $(0, 1)$, taking $x_n(\alpha) = 4 \log(n) - \log(\alpha)$,*

- **Rank-1 statistic**

$$\mathbb{P} \left(\exists \tau < n \in \mathbb{N} \quad s.t. \quad S_{\tau,n}^{\#1} > 2x_n(\alpha) + 2 \log(2p) \right) \leq \alpha.$$

- **Rank-p statistic**

$$\mathbb{P} \left(\exists \tau < n \in \mathbb{N} \quad s.t. \quad S_{\tau,n}^{\#p} > 2x_n(\alpha) + 2\sqrt{px_n(\alpha)} + p \right) \leq \alpha;$$

- **Thresholded statistic**

$$\mathbb{P} \left(\exists \tau < n \in \mathbb{N} \quad s.t. \quad S_{\tau,n}^{(a)} > 4x_n(\alpha) + 6pe^{-a^2/8} \right) \leq \alpha.$$

- **Rank-s statistic**

$$\mathbb{P} \left(\exists \tau < n \in \mathbb{N} \quad s.t. \quad S_{\tau,n}^{\#s} > 2(x_n(\alpha) + \log \binom{p}{s}) + 2\sqrt{s(x_n(\alpha) + \log \binom{p}{s}) + s} \right) \leq \alpha;$$

Proof. For all statistics, the proof follows the peeling argument of Lemma 8 in Yu et al. [2023]. In detail, for some generic statistic $\tilde{S}_{\tau,n}$ and some non-decreasing b_n , we can bound the probability of the event $\exists \tau < n \in \mathbb{N}$ such that $\tilde{S}_{\tau,n} > b_n$ using two union bounds:

$$\begin{aligned}
\mathbb{P}\left(\exists \tau < n \in \mathbb{N} \text{ such that } \tilde{S}_{\tau,n} > b_n\right) &\leq \sum_{j=1}^{\infty} \mathbb{P}\left(\exists \tau < n \in [2^j, 2^{j+1}) \text{ such that } \tilde{S}_{\tau,n} > b_n\right) \\
&\leq 3 \sum_{j=1}^{\infty} 2^{2j-1} \max_{\substack{2^j \leq n < 2^{j+1} \\ 1 \leq \tau < n}} \mathbb{P}\left(\tilde{S}_{\tau,n} > b_n\right) \\
&\leq 3 \sum_{j=1}^{\infty} 2^{2j-1} \max_{1 \leq \tau < 2^j} \mathbb{P}(\tilde{S}_{\tau,2^j} > b_{2^j}).
\end{aligned}$$

We get the second inequality bounding the number of couples (τ, n) such that $\tau < n$ with n in $[2^j, 2^{j+1})$, there are:

$$\frac{(2^{j+1} - 2^j)(2^{j+1} - 2^j - 1)}{2} + (2^{j+1} - 2^j)^2 = 2^{j-1}(3 \times 2^j - 1).$$

We obtain the last equality using the fact that $n \rightarrow b_n$ is an increasing bound and that all the $\tilde{S}_{\tau,n}$ have the same distribution, meaning that $n \rightarrow \mathbb{P}(\tilde{S}_{\tau,n} > b_n)$ is non-increasing. To continue, we consider some appropriate concentration bound on all $\tilde{S}_{\tau,n}$ of the form $\mathbb{P}(\tilde{S}_{\tau,n} \geq c(x)) \leq e^{-x}$. To be specific:

- For the rank-1 statistic we take

$$P(S_{\tau,n}^{\#1} \geq c(x)) \leq e^{-x}, \quad (22)$$

with $c(x) = 2x + 2 \log(p) + 2 \log(2)$ which we obtain using a union bound over p univariate Gaussian random variable.

- For the rank-p and rank-s statistics we take

$$P(S_{\tau,n}^{\#s} \geq c(x)) \leq e^{-x}, \quad (23)$$

with $c(x) = s + 2\sqrt{s(x + \log \binom{p}{s})} + 2(x + \log \binom{p}{s})$ which we get from Lemma 1 of Laurent and Massart [2000] and a union bound over all $\binom{p}{s}$ choices of s dimensions out of p .

- For the threshold statistic we take

$$P(S_{\tau,n}^{(a)} \geq c(x)) \leq e^{-x}, \quad (24)$$

with $c(x) = 6pe^{-a^2/8} + 4x$ which we get from Lemma 17 of Chen et al. [2022].

Setting $b_{2^j} = c(\tilde{x}_{2^j}(\alpha))$, we remove the probability term using these concentration bounds to write:

$$\mathbb{P}\left(\exists \tau < n \in \mathbb{N} \text{ s.t. } \tilde{S}_{\tau,n} > b_n\right) \leq 3 \sum_{j=1}^{\infty} 2^{2j-1} \exp(-\tilde{x}_{2^j}(\alpha)).$$

Considering $\exp(\tilde{x}_{2^j}(\alpha)) = \frac{3}{\alpha} 2^{2^{j-1}} j(j+1)$ we get:

$$3 \sum_{j=1}^{\infty} 2^{2^{j-1}} \exp(-\tilde{x}_{2^j}(\alpha)) = \sum_{j=1}^{\infty} \frac{\alpha}{j(j+1)} = \alpha.$$

and we have the value for evaluating c given by:

$$\tilde{x}_n(\alpha) = 2 \log(n) - \log(\alpha) + \log(\log_2(n)(\log_2(n) + 1)) + \log\left(\frac{3}{2}\right) \leq 4 \log(n) - \log(\alpha) = x_n(\alpha),$$

using relation $2^{2^j} \geq \frac{3}{2} j(j+1)$ on integers for the inequality. As the function c is increasing, we can use the simpler value $x_n(\alpha)$ which leads to the proposed result. \square

We now provide some bounds to control the detection delay, assuming we know the pre-change mean and the threshold is fixed or concave increasing.

Lemma 8. *Consider a sequence with a change δ at τ^* , that is $y_t = \varepsilon_t$ for $t \leq \tau^*$ and $y_t = \delta + \varepsilon_t$ for $t > \tau^*$ and $\|\delta\| > 0$.*

- *Suppose the threshold $c_n = c$ is fixed and positive. Then for any*

$$n - \tau^* \geq \frac{2c - 8 \log(\alpha/2)}{\|\delta\|^2} = \Delta(\delta, c, \alpha)$$

we have

$$\mathbb{P}\left(\left\|\frac{\sum_{t=\tau^*+1}^n y_t}{\sqrt{n - \tau^*}}\right\|^2 < c\right) \leq \alpha.$$

- *Suppose the threshold $c_n = c$ is fixed, positive and larger than p . Then for any*

$$n - \tau^* \geq \frac{2(c - p) + 4\sqrt{p \log(3/\alpha)} - 8 \log(\alpha/3)}{\|\delta\|^2} = \Delta'(\delta, c, \alpha, p)$$

we have

$$\mathbb{P}\left(\left\|\frac{\sum_{t=\tau^*+1}^n y_t}{\sqrt{n - \tau^*}}\right\|^2 < c\right) \leq \alpha.$$

- *Suppose the threshold c_n is increasing, concave and its derivative c'_n well-defined for all integers n . Then for any $n - \tau \geq \Delta(\delta, c_{\tau^*}, \alpha) + 2 \frac{c'_{\tau^*}}{\|\delta\|^2}$ we have*

$$\mathbb{P}\left(\left\|\frac{\sum_{t=\tau^*+1}^n y_t}{\sqrt{n - \tau^*}}\right\|^2 < c_n\right) \leq \alpha.$$

Proof. We define $u_n = \sum_{t=\tau+1}^n \langle \frac{\delta}{\|\delta\|}, \varepsilon_t \rangle$. Note that u_n is $\mathcal{N}(0, 1)$.

We get

$$\begin{aligned}
\left\| \frac{\sum_{t=\tau+1}^n y_t}{\sqrt{n-\tau}} \right\|^2 &= \left\| \sqrt{n-\tau} \delta + \frac{\sum_{t=\tau+1}^n \varepsilon_t}{\sqrt{n-\tau}} \right\|^2 \\
&= (n-\tau) \|\delta\|^2 + 2\|\delta\| \sum_{t=\tau+1}^n \left\langle \frac{\delta}{\|\delta\|}, \varepsilon_t \right\rangle + \left\| \frac{\sum_{t=\tau+1}^n \varepsilon_t}{\sqrt{n-\tau}} \right\|^2 \\
&\geq (n-\tau) \|\delta\|^2 + 2\|\delta\| u_n \\
&\geq (\sqrt{n-\tau} \|\delta\| + u_n)^2 - u_n^2.
\end{aligned}$$

Thus, we have:

$$\begin{aligned}
(n-\tau) \|\delta\|^2 \geq \left(\sqrt{c_n + u_n^2} - u_n \right)^2 &\iff (\sqrt{n-\tau} \|\delta\| + u_n)^2 - u_n^2 \geq c_n \\
&\implies \left\| \frac{\sum_{t=\tau+1}^n y_t}{\sqrt{n-\tau}} \right\|^2 \geq c_n.
\end{aligned} \tag{25}$$

Using the fact that for any (a, b) in \mathbb{R}^2 , $2a^2 + 2b^2 \geq (a-b)^2$ we get

$$(n-\tau) \|\delta\|^2 \geq 2c_n + 4u_n^2 \implies (n-\tau) \|\delta\|^2 \geq \left(\sqrt{c_n + u_n^2} - u_n \right)^2.$$

In terms of probability events, we are looking for a delay $(n-\tau)$ such that the probability of detecting a change is greater than $1-\alpha$, this can be written as:

$$1-\alpha \leq \mathbb{P}\left((n-\tau) \|\delta\|^2 \geq 2c_n + 4u_n^2\right) \leq \mathbb{P}\left(\left\| \frac{\sum_{t=\tau+1}^n y_t}{\sqrt{n-\tau}} \right\|^2 \geq c_n\right).$$

It is known that u_n is $\mathcal{N}(0, 1)$ and that $1-\alpha \leq \mathbb{P}(-2\log(\alpha/2) > u_n^2)$ so we solve for a fixed threshold $c_n = c$: $-8\log(\alpha/2) \leq (n-\tau) \|\delta\|^2 - 2c$, leading to the relation:

$$n-\tau \geq \frac{2c - 8\log(\alpha/2)}{\|\delta\|^2}.$$

For the second result, we proceed similarly but including a lower bound on $\left\| \frac{\sum_{i=\tau+1}^n \varepsilon_i}{\sqrt{n-\tau}} \right\|^2$ using Laurent and Massart [2000]

$$\left\| \frac{\sum_{i=\tau+1}^n \varepsilon_i}{\sqrt{n-\tau}} \right\|^2 \geq p - 2\sqrt{p \log(3/\alpha)}.$$

For the third result, we use the concavity property: $c_n \leq c_{n_0} + (n-n_0)c'_{n_0}$ in order to write:

$$-8\log(\alpha/2) + 2c_n \leq -8\log(\alpha/2) + 2(c_{n_0} + (n-n_0)c'_{n_0}) \leq (n-\tau) \|\delta\|^2.$$

If the second inequality is true, the full line is true, which leads to the result with $n_0 = \tau$. Notice that the bound c_n is often chosen proportional to $\log(n)$ such that the delay found with constant c_n is shifted by a constant when $\|\delta\|^2 \geq \frac{1}{n_0} \frac{n-n_0}{n-\tau}$.

□

J Acknowledgements and Funding

This work was supported by EPSRC grants EP/Z531327/1, EP/W522612/1 and EP/N031938/1 and an ATIGE grant from Génopole. The IPS2 benefit from the support of Saclay Plant Sciences-SPS [ANR-17-EUR-0007]